B. TECH. PROJECT REPORT

ON

AEROFOIL STRUCTURAL ENHANCEMENT THROUGH EMBEDDED CNTS

BY

R Harsh

DISCIPLINE OF MECHANICAL ENGINEERING

INDIAN INSTITUTE OF TECHNOLOGY INDORE

November 2023

Aerofoil Structural Enhancement through Embedded CNTs

A PROJECT REPORT

Submitted in partial fulfillment of the
requirements for the award of the degrees

of

BACHELOR OF TECHNOLOGY

in

MECHANICAL ENGINEERING

Submitted by:

R Harsh

Guided by:

Dr. Shailesh I Kundalwal

Associate Professor

Department of ME

IIT Indore

INDIAN INSTITUTE OF TECHNOLOGY INDORE

November 2023

CANDIDATE'S DECLARATION

I hereby declare that the project entitled **"Aerofoil Structural Enhancement through Embedded CNTs"** submitted in partial fulfillment for the award of the degree of Bachelor of Technology in 'Mechanical Engineering' completed under the supervision of Dr. Shailesh I Kundalwal, Associate Professor, IIT Indore is an authentic work.

Further, I/we declare that I/we have not submitted this work for the award of any other degree elsewhere.

Harsh
27/11/23

R Harsh

CERTIFICATE by BTP Guide(s)

It is certified that the above statement made by the students is correct to the best of my/our knowledge.

(SI Kundalwal)

27/11/2023

Dr. Shailesh I Kundalwal

Associate Professor

Department of ME

IIT Indore

Preface

This report on “Aerofoil Structural Enhancement through Embedded CNTs” is prepared under the guidance of Prof. Shailesh I Kundalwal.

The aviation industry has witnessed remarkable advancements in materials science, engineering, and design, leading to the development of aircraft with improved performance, efficiency, and sustainability. This research paper delves into the intricacies of the wing structure of the Airbus A320, a prominent workhorse in commercial aviation, with a particular focus on the incorporation of carbon fiber and the subsequent enhancement through the integration of carbon nanotubes.

The choice of materials in aerospace engineering plays a pivotal role in shaping the structural integrity and performance of an aircraft. Carbon fiber, characterized by its exceptional strength-to-weight ratio, has become a cornerstone in modern aviation design. This research endeavors to unravel the specific parameters governing the wing structure of the Airbus A320 when constructed with carbon fiber, exploring its mechanical properties, stress distribution, and overall structural behavior. As technology continues to advance, the aerospace community is increasingly turning its attention to nanomaterials for further enhancements. Carbon nanotubes, with their extraordinary mechanical, thermal, and electrical properties, present an exciting avenue for augmenting the capabilities of traditional materials. This paper embarks on a journey to investigate the synergistic effects of introducing carbon nanotubes into the carbon fiber structure of the Airbus A320 wing, seeking to unveil potential improvements in strength, flexibility, and overall performance. Throughout this research endeavor, we have drawn inspiration from the pioneers in materials science, the engineers who push the boundaries of what is possible, and the shared vision of a more sustainable and efficient aviation future.

This preface serves as an introduction to the comprehensive exploration that follows, providing readers with insights into the motivation, scope, and objectives of the research. As we navigate the realms of carbon fiber, carbon nanotubes, and the intricate design considerations of the Airbus A320 wing, we invite readers to join us in unraveling the potential advancements that lie at the intersection of materials innovation and aerospace engineering

R Harsh
B.Tech. IV Year
Discipline of Mechanical Engineering
IIT Indore

Acknowledgements

I wish to thank Dr. Shailesh I Kundalwal, Dr. Madhur Gupta for their kind support and valuable guidance. Their research expertise in the field of composite material sciences and previously published resources have been the core driving forces that have contributed to my research. Their expertise in the field of CNT integration of CFRPs has been a beacon of innovation. Their pioneering work in understanding the synergies between these materials has offered critical insights that have directly informed the methodologies and approaches adopted in my own research. I am sincerely grateful to both Dr. Shailesh I Kundalwal and Dr. Madhur Gupta for generously sharing their knowledge, offering guidance, and fostering an environment of collaborative learning. Their published resources on composite materials have undoubtedly left an indelible mark on the trajectory of my research.

R Harsh
B.Tech. IV Year
Discipline of Mechanical Engineering
IIT Indore

Abstract

This project attempts to draw conclusive evidence of Carbon Fiber composite reinforcement by integration of Epoxy Embedded Carbon Nanotubes (CNTs) and studying its application in the Aerospace Industry. Carbon Fibers are used in the aerospace industry increasingly, but their potential in this field has plateaued, hence this project tries to explore the integration of CNTs in the Carbon Fiber Structures of Aircrafts. This project utilizes the Finite Element Method (FEM) and Computational Fluid Dynamics (CFD) to run the numerical analysis of the Wing, which would be designed in the CAD Software Fusion 360.

We first Design the airplane using Airbus A320 Standards. During CFD Simulations we conduct a validation checks of 2D Aerofoil and then move onto 3D CFD Simulation of the aircraft wings to find the required force input parameters. The composite model is then created in ACP PrePost with different orientations of the underlying fabric with industry standard metal allocations to internal structure. Static Structural Analysis and Modal Analysis is now done to find parameters that define structural integrity. An explicit dynamic analysis is done for the aircraft in the form of a crash/strike testing using LS-DYNA. Now the required composite reinforcement is fabricated using CNTs embedded into Epoxy with different positions and orientations. This new material is then reapplied to every component in the system that contains Carbon Fiber Composite and the same analyses are conducted to retrieve new results. These new results are then compared to non-reinforced composite results to find the structural enhancement contributed by CNTs. This Enhancement is employed to find the potential benefits accessible and to subjugate the short-comings of previous composite models and their failures.

Table of Contents

B. TECH. PROJECT REPORT 1

CANDIDATE'S DECLARATION 3

CERTIFICATE by BTP Guide(s) 3

Preface 4

Acknowledgements 5

Abstract 6

Table of Contents 7

List of Figures 10

List of Tables 12

Chapter 1 - Introduction 13

1.1 Mechanical and Materials Design 13

1.2 Composite Materials 13

1.3 CAD Designing 13

1.4 Computer Aided Engineering (CAE) 14

Chapter 2 - Literature Review 15

2.1 A320 Aircraft Characteristics: 15

2.2 Airfoil Tools Database List: 15

2.3 Turbulence Modelling Resource: 15

2.4 Modelling and Structural Analysis of Three-Dimensional Wing: 16

2.5 Modelling and Finite Element Analysis of an Aircraft Wing using Composite Laminates: 17

2.6 Design and Analysis of A320 Wing using E-Glass Epoxy Composite: 17

2.7 Finite element analysis of aircraft wing using carbon fibre reinforced polymer and glass fibre reinforced polymer: 17

2.8 Influence of CNT waviness on the effective Young's modulus of multiscale hybrid composite: 18

2.9 Effect of orientation of CNTs and piezoelectric fibres on the damping performance of multiscale composite plate: 18

Chapter 3 - Methodology 19

3.1 Fusion 360 19

3.2 ANSYS Fluent 19

3.3 ANSYS Mechanical 21

Chapter 4 - Simulation and Analytical Modelling Details 23

4.1 3D CAD Modelling 23

4.2 2D CFD Validation Check 25

4.3 3D CFD Simulations 27

4.4 CFD To FEA Parameter Input 30

4.5 ANSYS Composite PrePost 31

4.6 Static Structural Analysis 33

4.7 Modal Analysis 35

4.8 Explicit Dynamic Analysis (LS-DYNA) 36

4.9 CNT Integration 37

Chapter 5 - Results and Discussion 38

5.1 Fusion 360 38

5.2 2D CFD Analysis 39

5.3 3D CFD Simulations 41

5.4 CFD To FEA Verification 43

5.5 ANSYS Composite PrePost 44

5.6 Static Structural Analysis 44

5.7 Modal Analysis 45

5.8 Explicit Dynamic Analysis 47

Chapter 6 - Conclusion and Future Scope 49

6.1 Conclusion 49

6.2 Future Scope 51

References 52

List of Figures

Figure 1: NACA 23015 Airfoil Profile 15
Figure 2: A320 Wing Inner Structure 16
Figure 3: Revolve Command 23
Figure 4: Loft Command 23
Figure 5: Sweep Command 23
Figure 6: Combine and Split Commands 24
Figure 7: Dimensions in the Front and Side View 24
Figure 8: Dimensions in the Top View 24
Figure 9: Green Highlighted Airfoil with Fluid Domain 25
Figure 10: Meshing of the 2D Domain 26
Figure 11: Orthogonality 26
Figure 12: Aspect Ratio 26
Figure 13: Mesh Statistics 26
Figure 14: Meshing of the 3D Fluid Domain 27
Figure 15: Inflation at the Surface of the Airfoil 28
Figure 16: Aspect Ratio of elements. 28
Figure 17: Element Quality of Fluid Domain 28
Figure 18: Mesh Statistics 29
Figure 19: Flow Chart of the Setup Steps 29
Figure 20: Project Schematic of CFD & FEA Validation 30
Figure 21: Mesh of Airfoil at Tip Chord 31
Figure 22: Element Quality 31
Figure 23: Aspect Ratio 32
Figure 24: Polar Properties of Ply A, Ply B, Ply C Respectively 32
Figure 25: Mesh of Non-Composite model at Tip 33
Figure 26: Element Quality 33
Figure 27: Aspect Ratio 33
Figure 28: Boundary Conditions Applied 34
Figure 29: Details of Modal Pre-Analysis Settings 35
Figure 30: Project Schematic of ACP, Static Structural, Modal analyses 35
Figure 31: LS - DYNA Project Schematic 36

Figure 32: LS - DYNA Analysis Settings 36
Figure 33: Pre CNT-Integration Material Properties 37
Figure 34: Post CNT-Integration Material Properties 37
Figure 35: Isometric View 38
Figure 36: Top View and Front View 38
Figure 37: Coefficient of Lift 39
Figure 38: Coefficient of Drag 39
Figure 39: Velocity and Pressure Contours 39
Figure 40: Total Kinetic Energy Contour and Velocity Vectors 40
Figure 41: Plot of Cp with Experimental Validation 40
Figure 42: Lift Force vs. Iterations 41
Figure 43: Drag Force vs. Iterations 41
Figure 44: Velocity and Pressure Contours 42
Figure 45: Streamlines 42
Figure 46: Scaled Residuals 42
Figure 47: CFD And Manually Applied Force Deformation 43
Figure 48: CFD And Manually Applied Force Stresses 43
Figure 49: Inverse Reserve Factor 44
Figure 50: Total Deformation 44
Figure 51: Equivalent Stresses 45
Figure 52: Mode Shapes 1, 2 and 3 45
Figure 53: Mode Shapes 4, 5 and 6 45
Figure 54: Equivalent Stress Contour at the End of Crash 47
Figure 55: Stress Contour for Non-Composite Material 47
Figure 56: Equivalent Stresses for Composite Fabric 47
Figure 57: Ply A: Regular and CNT Integrated 48
Figure 58: Ply B: Regular and CNT Integrated 48
Figure 59: Ply C: Regular and CNT Integrated 48
Figure 60: Static Structural Analysis Result Comparison 50
Figure 61: Explicit Dynamic Analysis Results Comparison 50

List of Tables

Table 1: Aircraft Characteristics 15

Table 2: Airbus A320 Specifications 16

Table 3: Material Selection 16

Table 4: Ply Specification 17

Table 5: Misc Specifications 17

Table 6: Effective Properties concluded from Both References 18

Table 7: Boundary Conditions Applied 34

Table 8: Validation Check 40

Table 9: 3D CFD Results 43

Table 10: CFD and Manual Application Parameter Comparison 43

Table 11: ACP Post Results 44

Table 12: Static Structural Analysis Results 45

Table 13: Modal Analysis Results (Deformation in m and Frequency in Hz) 46

Table 14: Explicit Dynamic Analysis Results 48

Chapter 1 - Introduction

1.1 Mechanical and Materials Design

Mechanical and material design plays a pivotal role in the aerospace industry, particularly when it comes to composite materials. The unique demands of aerospace applications necessitate materials that are not only lightweight but also possess exceptional strength and durability. Composite materials, such as carbon fiber integrated with carbon nanotubes, offer a compelling solution to meet these criteria. The intricate design and selection of materials directly impact an aircraft's structural integrity, fuel efficiency, and overall performance. Innovations in mechanical and material design empower engineers to create aircraft with reduced weight, enhanced strength, and improved fuel efficiency, thus contributing significantly to the advancement and sustainability of the aerospace industry.

1.2 Composite Materials

Composite materials in aerospace engineering involve combining two or more distinct materials to create a stronger and more lightweight structure. Carbon fiber, a key player in modern aviation, consists of thin strands of carbon tightly woven and infused with resin. Today, carbon fiber is extensively used in aircraft design, contributing to reduced weight, increased fuel efficiency, and enhanced overall performance in the dynamic and demanding field of aerospace engineering.

1.3 CAD Designing

CAD stands for Computer Aided Design, which is a way to create 3D models of objects which can be further used to perform certain tasks on it like 3D Printing or Simulations like FEM and CFD. This method has been used in this paper to create models of Airbus A320 and its Wing Structure. Which can be further used to conduct CFD analyses and FEM Structural, Modal and Explicit Dynamic Analyses. The CAD software used here is Fusion 360 due to its friendly GUI layout and various applications in other aspects of Engineering

1.4 Computer Aided Engineering (CAE)

Computer Aided Engineering is a way of simulating real-life conditions and cases into a computer to find the required parameters and obtain post processing results in a visually appealing and intuitive way. The methods used in this paper are CFD and FEM. The software used in this paper is ANSYS Mechanical Version 2023 R1.

1.4.1 Computational Fluid Dynamics (CFD)

CFD is a discipline using numerical methods to simulate fluid flow and heat transfer. It employs algorithms to solve equations representing fluid behavior, providing insights into complex interactions. Applied in aerospace and engineering, CFD aids in optimizing designs and predicting fluid dynamics.

1.4.2 Finite Element Method

FEM is a numerical technique breaking down structures into elements for analysis. It models interactions between elements, predicting stress, strain, and deformation. Widely used in engineering, FEM ensures structural integrity and aids in design optimization across various applications. FEM analyses used in this paper are Static Structural, Modal and Explicit Dynamic Analyses.

Chapter 2 - Literature Review

2.1 A320 Aircraft Characteristics:

Airbus A320 Dimensional Specifications, Maximum Take-Off Weight (MTOW) = 77000 kg, Maximum Landing Weight (MLW) = 64500 kg, Turbine Specifications IAE V2500, Maximum Taxi Weight (MTW) = 77400 kg, Maximum Ramp Weight (MRW) = 77400 kg, Maximum Zero Fuel Weight (MZFW) = 61000 kg.

Author: Airbus, https://aircraft.airbus.com/

Aircraft Characteristics	
	WV010
Maximum Ramp Weight (MRW) Maximum Taxi Weight (MTW)	77 400 kg (170 638 lb.)
Maximum Take-Off Weight (MTOW)	77 000 kg (169 756 lb.)
Maximum Landing Weight (MLW)	64 500 kg (142 198 lb.)
Maximum Zero Fuel Weight (MZFW)	61 000 kg (134 482 lb.)

Table 1: Aircraft Characteristics

2.2 Airfoil Tools Database List:

NACA 23015 Airfoil Profile as CSV Spline Import with chord length of 4m, which is then input into CAD Software Fusion 360 to create a sketch for 2D CFD Analysis and 3D Wing Structure recreation.

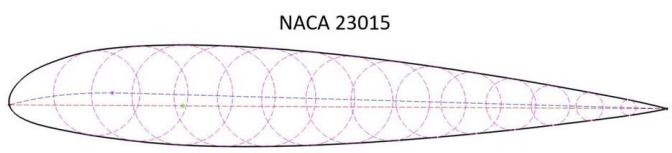

Figure 1: NACA 23015 Airfoil Profile

Author: Airfoil Tools Website, https://airfoiltools.com/search/

2.3 Turbulence Modelling Resource:

Values of C_L and C_D to conduct a Validation check on the 2D CFD analysis in ANSYS Fluent on the used NACA Profile.

Author: Langley Research Centre, NASA, https://turbmodels.larc.nasa.gov/

2.4 Modelling and Structural Analysis of Three-Dimensional Wing:

Maximum Mach Operating Speed (MMO) = 0.82, Cruise Speed = 0.79 – 0.80, Wing Structure, Rib Specifications, Material Allotment.

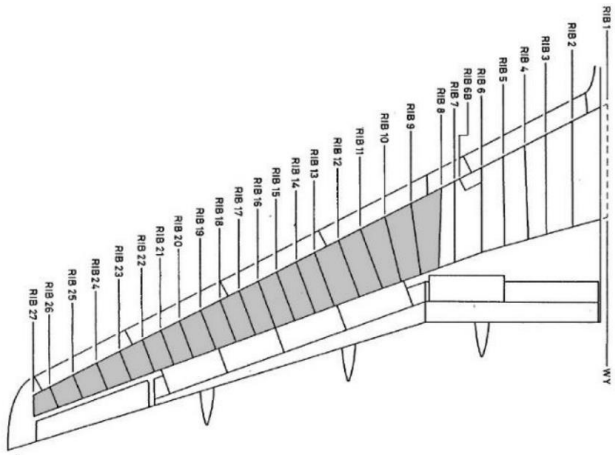

Figure 2: A320 Wing Inner Structure

Airbus A320		
Airfoil	Root Airfoil	NACA 23015
	Kink Airfoil	NACA 5 - Digit
	Kink Airfoil	NACA 5 - Digit
	Root Chord Length	7.05 m
	Tip Chord Length	1.50 m
Skin Thickness		9.1 mm
Spar	Position of Front Spars	0.2 m
	Position of Rear Spars	0.65 m
Operating Limit Speed	MMO	0.82
	Cruise Speed	0.79 – 0.80

Table 2: Airbus A320 Specifications

Airbus A320 Materials	
Wing Component	**Material Selection**
Ribs	Aluminium Alloy
Wing Skin	Epoxy Carbon Fibre (395 GPa)
Primary and Secondary Spars	Titanium Alloy

Table 3: Material Selection

2.5 Modelling and Finite Element Analysis of an Aircraft Wing using Composite Laminates:

Composite Material Selection (Epoxy Woven Carbon Fiber (395 GPa)), Ply Sequence (Thickness = 1mm), Ply Orientation.

Ply Specification	
Ply Name	**Ply Orientation**
Ply A	0/90/0/90/0
Ply B	0/90/45/-45/0/-45/45/90/0
Ply C	0/-35/45/90/-45/0/45/90/-45/35/0

Table 4: Ply Specification

2.6 Design and Analysis of A320 Wing using E-Glass Epoxy Composite:

Airbus A320 Wing Skin Thickness values, i.e., Thickness = 1mm per layer in stack up. Totalling 5mm Ply A, 9mm Ply B and 11mm Ply C.

2.7 Finite element analysis of aircraft wing using carbon fibre reinforced polymer and glass fibre reinforced polymer:

Root Chord Thickness, Total Number of Mode Shapes, Number of Ribs, Spars.

Misc Specifications	
Root Chord Thickness	4 m
Number of Mode Shapes	6 No.
Number of Ribs	16 No.
Number of Spars	2 No.

Table 5: Misc Specifications

2.8 Influence of CNT waviness on the effective Young's modulus of multiscale hybrid composite:

Effective Youngs Modulus (E1, E2, E3), Shear Modulus (G12, G23, G13), in 3 Directions with Carbon Nanotube Reinforced Epoxy Woven Carbon Fibers, ω = 0.

2.9 Effect of orientation of CNTs and piezoelectric fibres on the damping performance of multiscale composite plate:

Similar to the previous paper, Effective Youngs Modulus (E1, E2, E3), Shear Modulus (G12, G23, G13), in 3 Directions with Carbon Nanotube Reinforced Epoxy Woven Carbon Fibers, ω = 0.

Effective Properties		
Property	**Value**	**Units**
Young's Modulus X Direction	126	GPa
Young's Modulus Y Direction	126	GPa
Young's Modulus Z Direction	20	GPa
Poisson's Ratio XY	0.05	-
Poisson's Ratio YZ	0.3	-
Poisson's Ratio XZ	0.3	-
Shear Modulus XY	6.64	GPa
Shear Modulus YZ	5.3	GPa
Shear Modulus XZ	5.3	GPa

Table 6: Effective Properties concluded from Both References

Chapter 3 - Methodology

3.1 Fusion 360

The model of the Airbus A320 is created in Fusion 360 with measurements from the official site of Airbus, with operations like Extrude, Loft, Sweep, Shell, Pull, Combine, etc. The measurements used are:

3.2 ANSYS Fluent

ANSYS Fluent is the project part of ANSYS Mechanical used for CFD simulations. Computational Fluid Dynamics (CFD) simulations involve dividing the fluid domain into discrete cells, applying mathematical equations like the continuity equation, Navier-Stokes Equation to represent fluid behavior, and solving these equations iteratively to predict fluid flow patterns, pressure distributions, and other relevant parameters. CFD here is used to predict the Coefficients of Lift, Coefficients of Drags, and net Lift and Drag Force.

3.2.1 Turbulent Flow Equations in 2D

Continuity Equations:

$$\frac{\partial u}{\partial x} + \frac{\partial \mathrm{v}}{\partial \mathrm{y}} = 0$$

Reynold's Averaged Continuity Equation / Reynold's Decomposition:

$$u = \overline{u} + u' \quad \Rightarrow \quad \frac{d\overline{u}}{dx} + \frac{d\overline{v}}{dy} = 0$$

1. 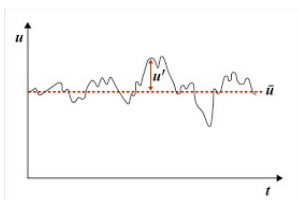

Reynold's Averaged Navier Stokes Equation:

$$\rho\frac{du}{dt} + \rho(u\frac{du}{dx} + v\frac{du}{dx}) = -\frac{dp}{dx} + \mu\nabla^2 u$$

Navier Stokes Equation

$$\rho\frac{d\overline{u}}{dt} + \rho(\overline{u}\frac{d\overline{u}}{dx} + \overline{v}\frac{d\overline{y}}{dx}) = -\frac{d\overline{p}}{dx} + \mu\nabla^2\overline{u} - \rho\,(\frac{\overline{u'du'}}{dx} + \frac{\overline{v'dx'}}{dy})$$

Reynold's Averaged Navier Stokes Equation

$$\rho(\overline{u}\frac{d\overline{u}}{dx} + \overline{v}\frac{d\overline{y}}{dx}) = -\frac{d\overline{p}}{dx} + \mu\nabla^2\overline{u} + \overline{f}_{turb,x}$$

Reynold's Averaged Navier Stokes Equation for Incompressible Fluids

$$\tau_{xy} = \mu(\frac{dv}{dx} + \frac{du}{dy})$$

$$\tau^t_{xy} = \mu_t(\frac{dv}{dx} + \frac{du}{dy})$$

$$\Downarrow$$

$$-\rho u'v'$$

K – Epsilon Model

K: Turbulent Kinetic Energy

Epsilon: Turbulent Dissipation (K dissipation)

$$\frac{\mu^t}{\rho} = \frac{C^\mu k^2}{\epsilon}$$

Dividing Domain into Control Volumes/Cells.

& Cell center values of the following are calculated.

$$\overline{u},\ \overline{v},\ \overline{\rho},\ k,\ \varepsilon$$

Coefficient of Lift (Thin Airfoil Theory):

$$C_l = \frac{Lift}{\frac{1}{2}\rho V_\infty^2 A} = 2\pi(\alpha - \alpha_\infty)$$

3.3 ANSYS Mechanical

3.3.1 Static Structural

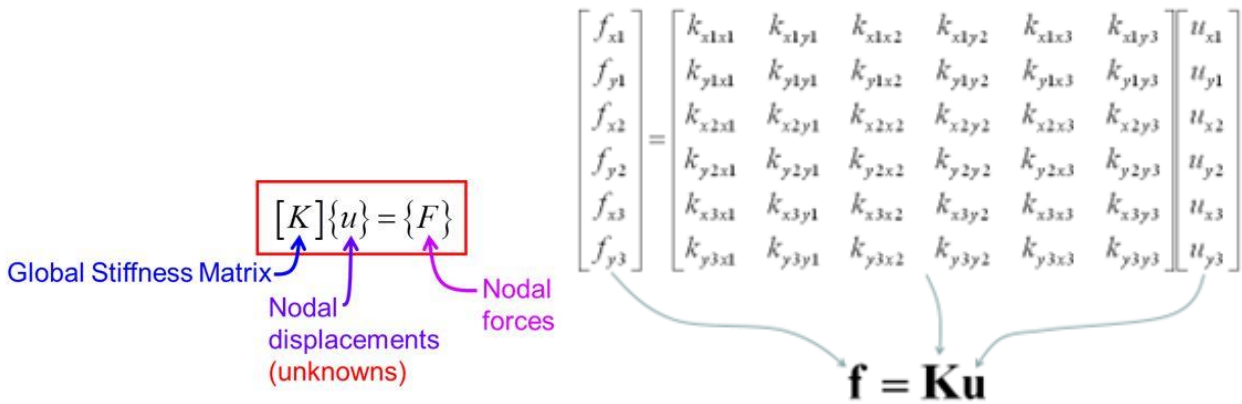

$\{F\}$ is "known" (load)

$[K]$ is "known" (geometry, material properties.... elements)

$\{U\}$ is to be determined (displacements)

This can be solved mathematically using a matrix inversion method

$\{F\} = [K]\{U\} \Rightarrow \{U\} = [K]^{-1}\{F\}$

Once the Displacements $\{U\}$ are known, then strains and stresses can be calculated:

$\varepsilon = \frac{\Delta u}{L}$(1D more complicated for 2D and 3D)

$\sigma = E.\varepsilon$

and FOS $= \frac{\sigma^y}{\sigma}$

3.3.2 Modal Analysis

$$F = [M].\ddot{x} + [C].\dot{x} + [K].x$$

[M]: Mass being accelerated

[C]: Damping Coefficient (Zero in current case)

[K]: Stiffness Matrix

$\ddot{x}$: Acceleration

$\dot{x}$: Velocity

x: Displacement

F: Load Force

$\Rightarrow$

Equation of Motion: $F = [M].\ddot{x} + [K].x$

Harmonic Solution: $x = \{\phi\}\sin(\omega t)$

Substituting: $([K] - \omega^2[M])\{\phi\} = 0$

ω = Frequency

ϕ = Mode Shapes

3.3.3 Explicit Dynamic Analysis

[M] {x''} + [C] {x'} + [k] {x} = {f}

Where x is displacement

If we try to solve governing equation for x value by using Implicit scheme

[K] {x} = {f} – ([M] {x''} + [C] {x'})

{X} = $[K]^{-1}$ ({f} - ([M] {x''} + [C] {x'}))

In Implicit scheme we need to do the inverse of stiffness for finding displacement

If we solve the same equation with explicit approach

[M]{x''} = {f} – ([C]{x'} + [K]{x})

$[M]^{-1}$ [M] {x''} = $[M]^{-1}$ ({f} – ([C]{x'} + [K]{x}))

{X''} = $[M]^{-1}$({f} – ([C]{x'} + [K]{x}))

In Explicit we need to do the inverse of Mass matrix and damping matrix for finding the displacement

$$\Delta t_{cr} = \frac{le}{c}, \; c = \sqrt{\frac{E}{\rho}}$$

Chapter 4 - Simulation and Analytical Modelling Details

4.1 3D CAD Modelling

4.1.1 Fuselage

3D CAD Modelling begins with creating a fuselage shape of the airplane using an extruded cross-section of the fuselage diameter to the net length of the aircraft. And then trimming of the excess material using Fusion 360 Operations like Revolve, Split Command, Shell, Taper Selection, Solid Loft. This involves a symmetric trim using the revolve command at the nose of the airplane, and a loft between two profiles, causing a tapered extrusion of profiles on a single side at the back-end of the airplane.

Figure 3: Revolve Command

Figure 4: Loft Command

4.1.2 Fins

The fins are created next using the same loft feature between two NACA 23015 Profiles with a separation of length of one Wing in between them. A fold of the airfoil is added to the end of the airplane which causes the breakage of turbulent stream and makes the aircraft more stable. This can be done using the Sweep Command.

Figure 5: Sweep Command

4.1.3 Combination

A final combination of all the different components is done after creating the bed of the fuselage where the fuselage attaches to the landing wheels (omitted here), This combination can be done with the combine command between two bodies and then attaching every body in a single component folder.

Figure 6: Combine and Split Commands

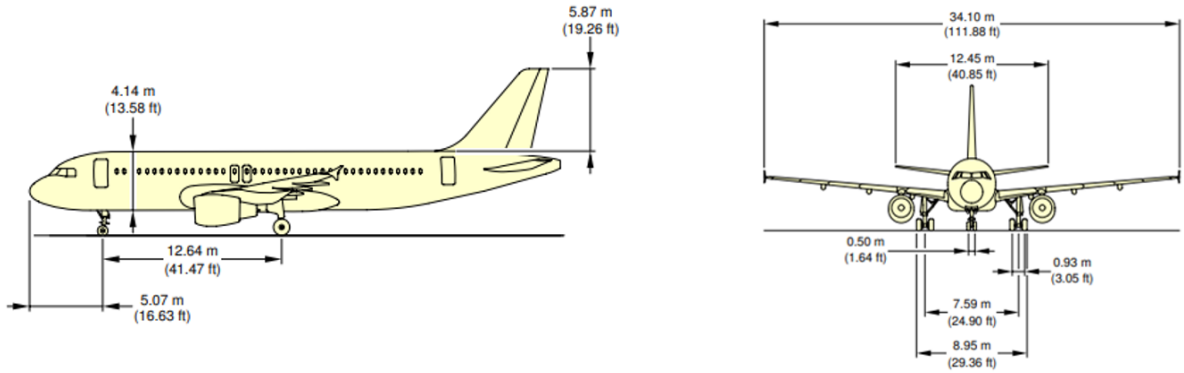

Figure 7: Dimensions in the Front and Side View

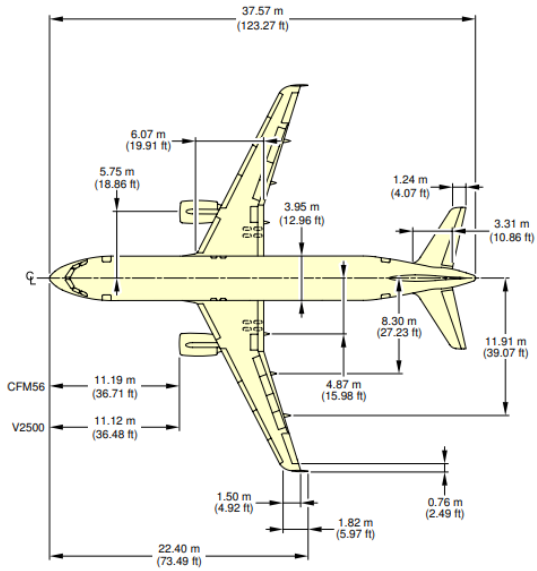

Figure 8: Dimensions in the Top View

4.2 2D CFD Validation Check

Before moving to 3D CFD Simulations, we must first validate our mathematical model of approach and cross-check with published resources, to confirm the reliability of our Simulation Model. This can be done by first performing a 2D CFD Validation check of the NACA 0012 Airfoil Profile. In ANSYS Project settings, Analysis type is set to be 2D.

4.2.1 Meshing

The fluid domain for 2D CFD Analysis is taken to be about 13 chord lengths (13xL) in front and behind the airfoils and to execute proper meshing for elements, inflation of 10 layers with a step of 1.2 near the airfoils surface is employed to properly account for the viscous boundary layers near the airfoil's outer region. In the end a spherical Body of Influence of 3x Chord Length is set from the Origin. We hope to achieve a high quality of mesh with a compromise in the calculation time elapse. This can be done by monitoring parameters like Aspect Ratio and Orthogonality.

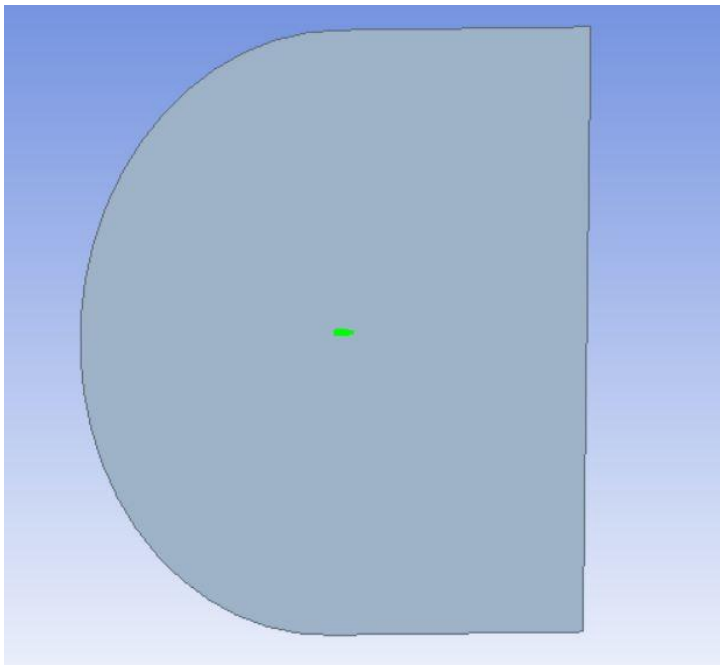

Figure 9: Green Highlighted Airfoil with Fluid Domain

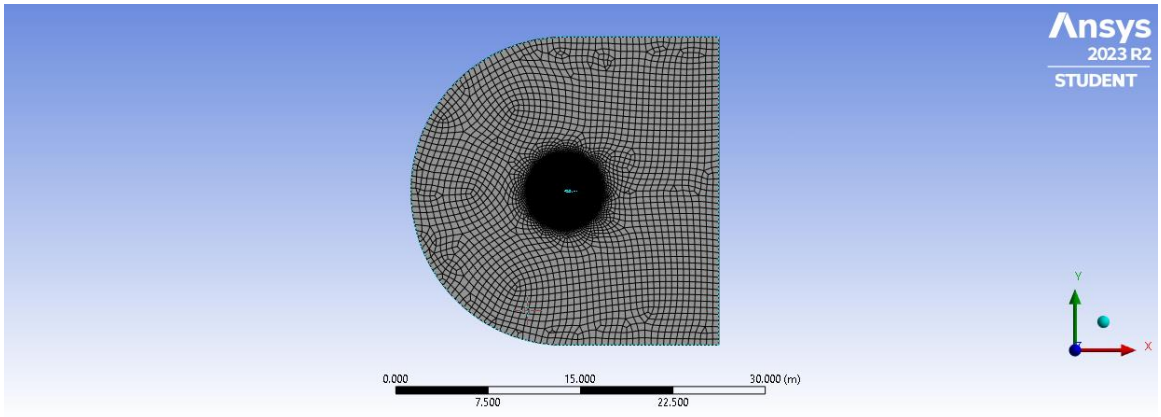

Figure 10: Meshing of the 2D Domain

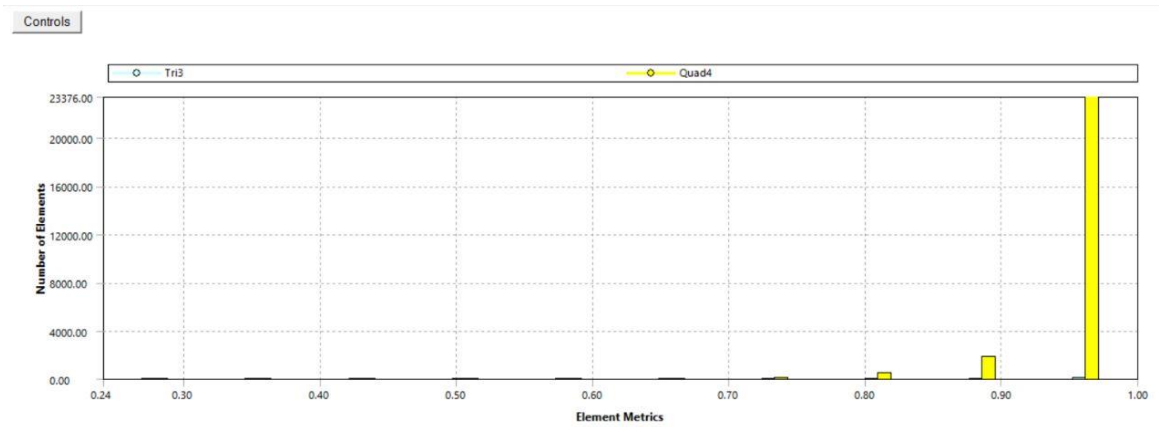

Figure 11: Orthogonality

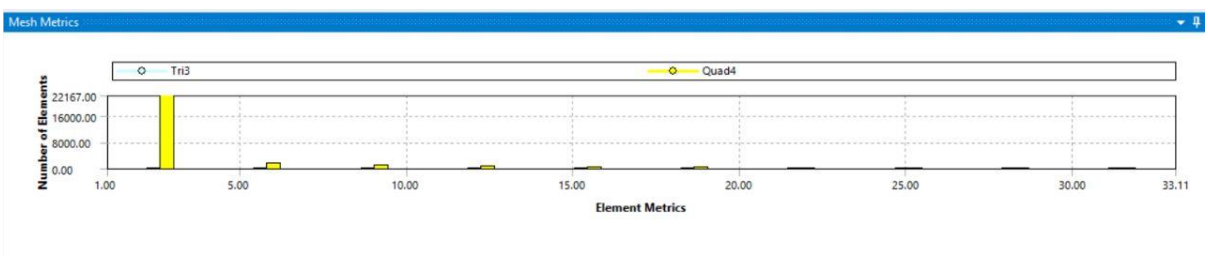

Figure 12: Aspect Ratio

Statistics	
Nodes	26315
Elements	25929
Show Detailed Statistics	Yes
Corner Nodes	26315
Shell Elements	25929
TriShell3	87
QuadShell4	25842

Figure 13: Mesh Statistics

4.2.2 Setup

In the "Setup" Section of the ANSYS workbench, ANSYS Fluent is opened and the first step is to check mesh. Then the solution method is set to k – ε Turbulence Model with the default values of k and ε.

Material Data is modified for air at the right altitude and temperature with $\rho = 1.1767$, $\mu = 1.009e\text{-}5$. Then boundary condition of Velocity Inlet is applied to leading bounds of the fluid domain with $V_{in} = 51.45$ m/s and angle of attack (AOA) is set to 10°. The top and bottom surface of the airfoil are set as "wall". Walls have "No-Slip" condition. And the trailing bounds of the fluid domain are set as the pressure outlet.

The final step is Initialization wherein initial guess values for the cell center parameters is set which is taken from lead bound of Fluid Domain and about 1000 Iterations are done to find convergence and extract the required Values of C_L and C_D.

4.3 3D CFD Simulations

After the validation check for the 2D CFD Simulations, we move onto the 3D CFD Analysis of the 3D Aircraft wing. The ANSYS Project setting of Analysis Type is left to be the default 3D. This time the 3D CAD Model of the Aircraft wing is to exported from Fusion 360 in the form of a STEP profile and a Boolean subtracting is done of the created Fluid domain and the model of the aircraft wing to get the isolated Fluid domain without the inclusion of aircraft wings.

4.3.1 Meshing

In the meshing of the 3D Model, Fluid Domain bounds are taken to be 3 times the chord length (3xL) with a 10-layer mesh inflation having a step of 1.2 to accurately simulate the fluid motion at the surface of the airfoil because of the viscous boundary layer. There is also a Rectangular Body of Influence set covering majority of the airfoil surface and focused on the trailing ends of the airfoil where most turbulence is found.

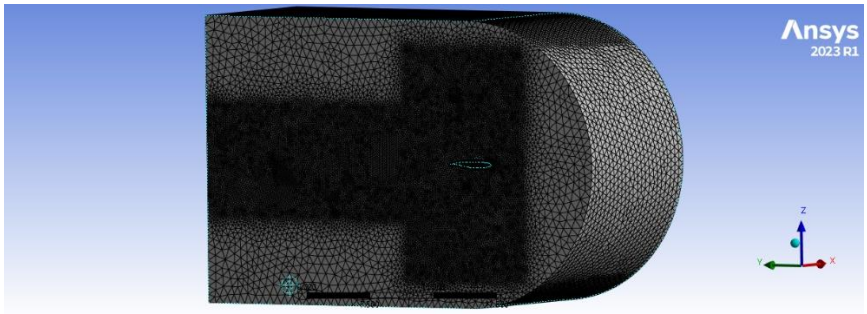

Figure 14: Meshing of the 3D Fluid Domain

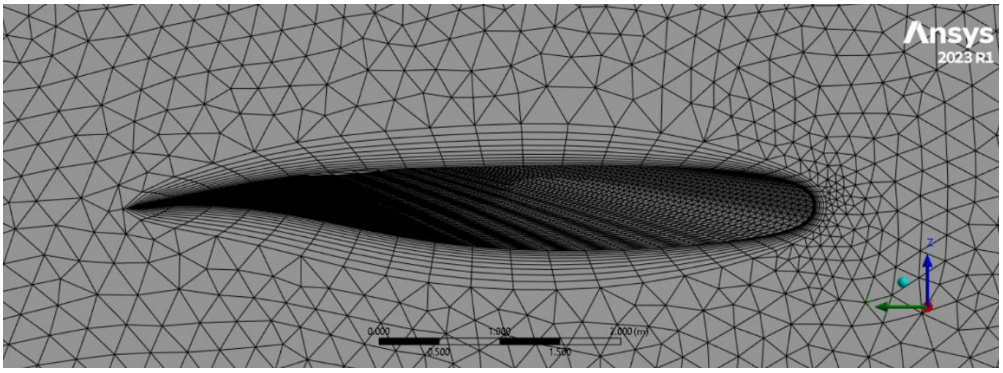

Figure 15: Inflation at the Surface of the Airfoil

Similar to the 2D CFD Simulations, Aspect Ratio, Element Quality of the Mesh is to be monitored.

Figure 16: Aspect Ratio of elements.

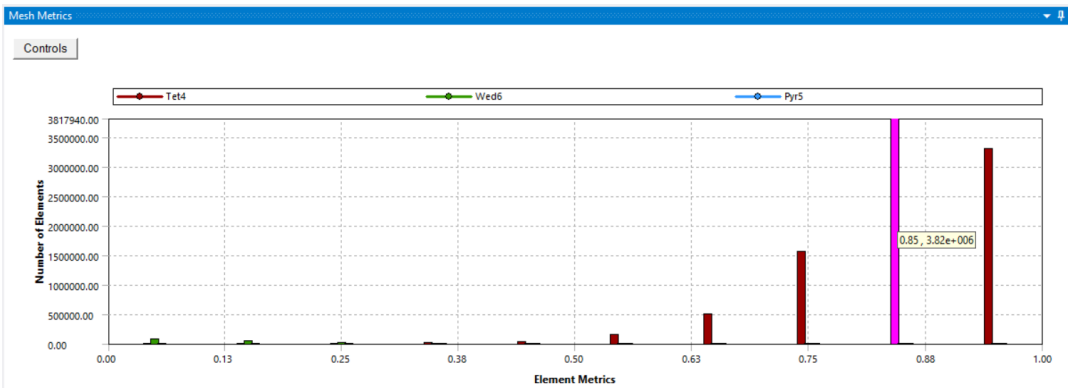

Figure 17: Element Quality of Fluid Domain

Statistics	
Nodes	1668830
Elements	9518088
Show Detailed Statistics	Yes
Corner Nodes	1668830
Solid Elements	9518088
Tet4	9371208
Wedge6	146400
Pyramid5	480

Figure 18: Mesh Statistics

4.3.2 Setup

In the "Setup" Section of the ANSYS workbench, ANSYS Fluent is opened and the first step is to check mesh. Then the solution method is set to k – ε Turbulence Model with the default values of k and ε.

Material Data is modified for air at the right altitude and temperature with ρ = 0.45, μ = 1.422e-5. This implies that Reynold's Number is around 1e6. Then boundary condition of Velocity Inlet is applied to leading bounds of the fluid domain with V_{in} = 246 m/s and angle of attack (AOA) is set to 10°. The top and bottom surface of the airfoil are set as "wall". Walls have "No-Slip" condition. And the trailing bounds of the fluid domain are set as the pressure outlet.

The final step is Initialization wherein initial guess values for the cell center parameters is set which is taken from lead bound of Fluid Domain and about 250 Iterations are done to find convergence and extract the required Values of Lift Force and Drag Force.

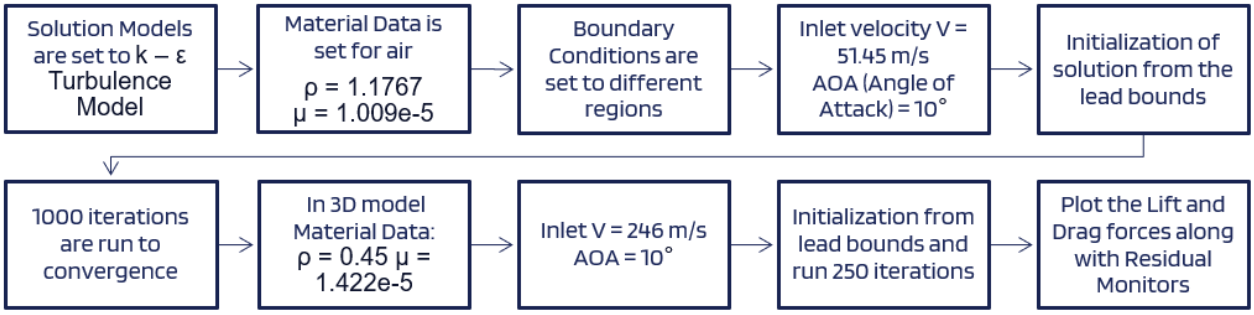

Figure 19: Flow Chart of the Setup Steps

4.4 CFD To FEA Parameter Input

One more validation check to be conducted is to verify the method of application of Lift Force on the airfoil profile. The results from the CFD simulations give a contour of the pressure applied but to confidently apply the lift force as a force distributed on the bottom surface of the airfoil, we need to verify the method we employ here. This can be done by linking the CFD Simulations to the Static Structural model of the Airfoil. A validation can then be done if the application of force as a surface force is around the equal of the pressure contoured force application from the CFD Results.

A Project Schematic for this can be seen here:

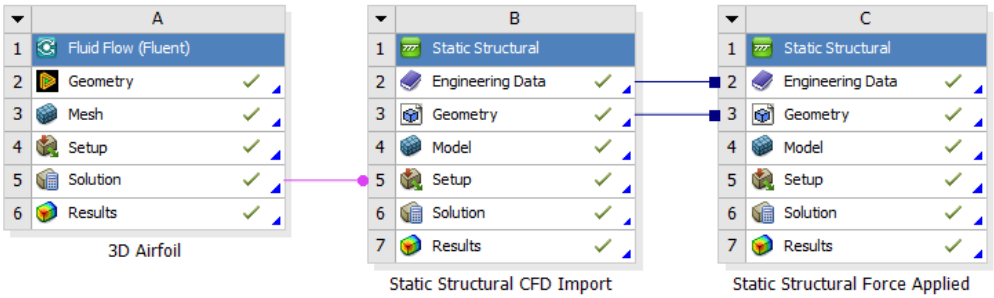

Figure 20: Project Schematic of CFD & FEA Validation

After the validation from this step, we can move onto the FEA consisting of Static Structural Analysis, Modal Analysis and Explicit Dynamic Analysis.

4.5 ANSYS Composite PrePost

To carry out the finite element analysis we need to first create a Carbon Fiber Stack-up with different orientations and assign proper material properties.

4.5.1 Mesh

To create the mesh, we first select a plane of working which in this case would be the outer surface of the wing, then we move to meshing of the wing with body sizing and face meshing to achieve an even mesh, for a tapered surface.

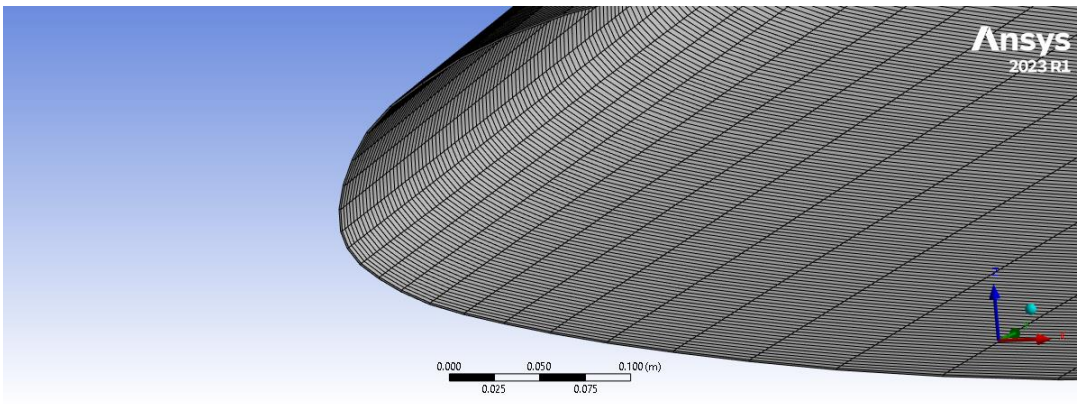

Figure 21: Mesh of Airfoil at Tip Chord

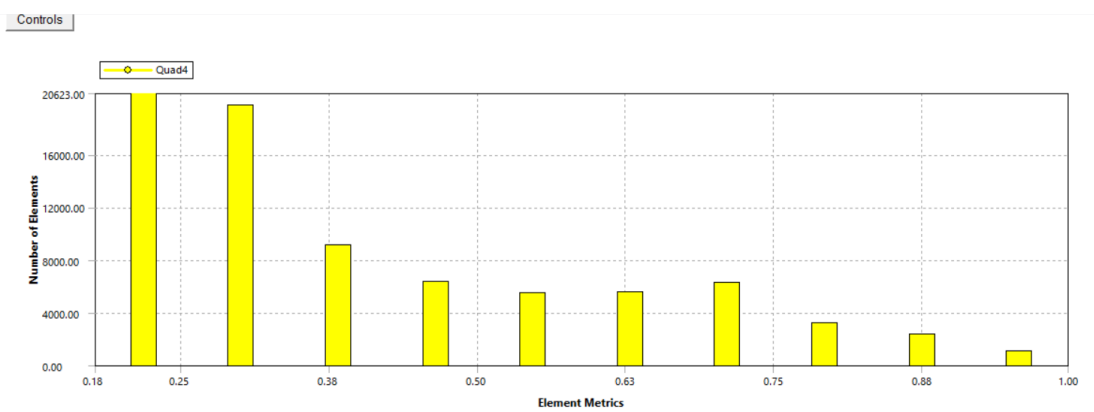

Figure 22: Element Quality

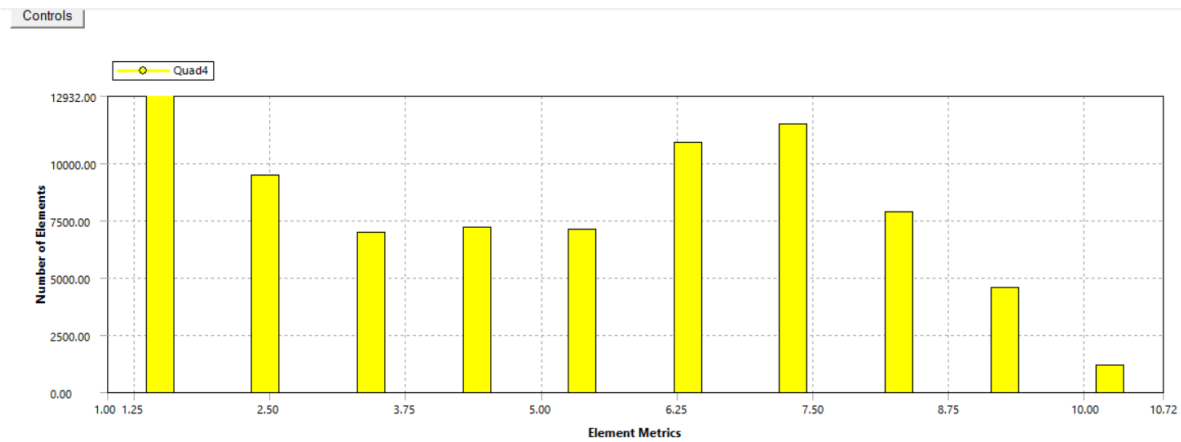

Figure 23: Aspect Ratio

4.5.2 Setup

In the setup, under the material data section, we create a Fabric of Carbon Fiber Woven Epoxy, with a thickness of 1mm. This fabric is then used to create a stack-up. In the Stack-up section we create a 5 Layer Stack-up for Ply A, 9 Layer Stack-up for Ply B and a 11 Layer Stack-up for Ply C, with the respective angular orientations. Then applying and updating the model, we get respective thicknesses for each composite material fabric. Their polar properties also vary accordingly.

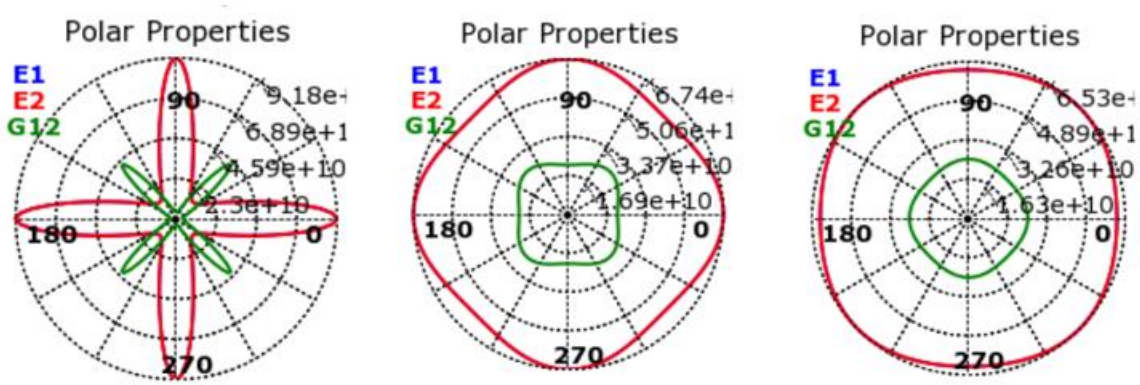

Figure 24: Polar Properties of Ply A, Ply B, Ply C Respectively

4.6 Static Structural Analysis

4.6.1 External Mechanical Model

There is a Mechanical Model Project used to assign material properties to the non-composite materials and mesh the resulting model. The mesh is kept fine to improve accuracy and the Meshing Method is set to be Hex Dominant to achieve even cuboidal mesh elements.

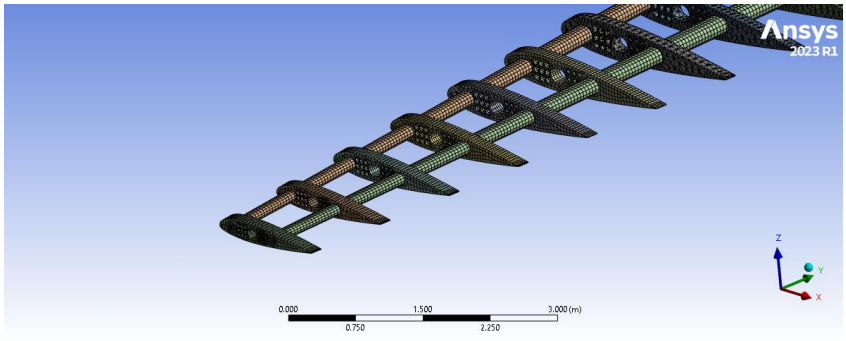

Figure 25: Mesh of Non-Composite model at Tip

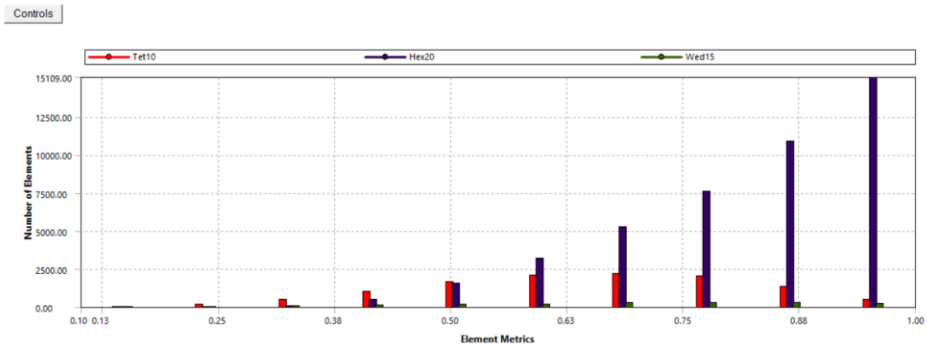

Figure 26: Element Quality

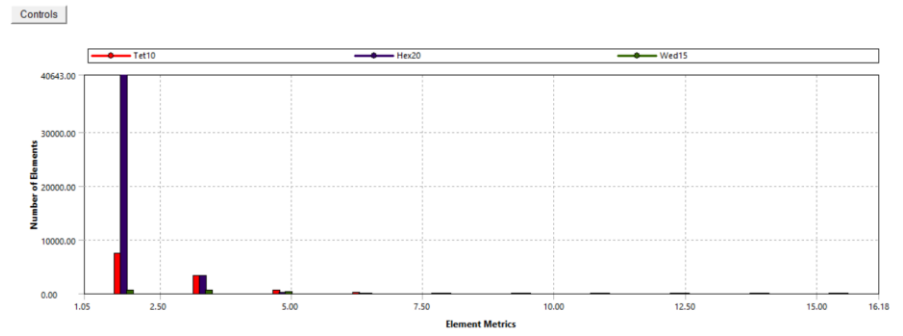

Figure 27: Aspect Ratio

4.6.2 Setup

Mesh:

The mesh part here is skipped due to the mesh being imported from ACP and the External Mechanical Model, causing the mesh to be ready. This mesh is also applied to further Finite Element Analyses i.e., Modal Analysis and the Explicit Dynamic Analysis.

Setup:

In the setup of static structural analysis, we apply boundary conditions to the model, like Fixed Supports, Load Forces etc. Some of these are angled at 10° due to the AOA.

The boundary conditions applied in this model are:

Boundary Conditions Applied		
Body Applied to	**Boundary Condition**	**Value**
Root Chord	Fixed Support	-
Bottom Surface	Lift Force	375.7 kN
Top and Bottom Surface	Drag Force	31 kN
4th Rib from Root	Turbine Weight	24.25 kN
Entire Body	Standard Earth Gravity	9.8066 m/s^2

Table 7: Boundary Conditions Applied

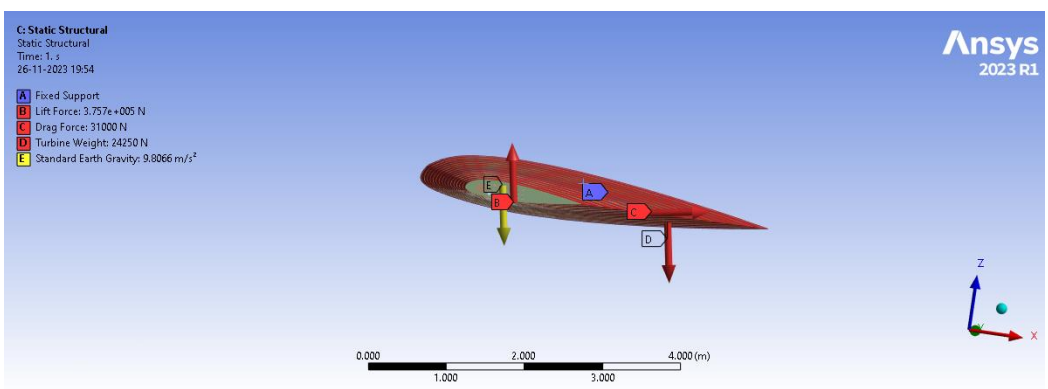

Figure 28: Boundary Conditions Applied

4.7 Modal Analysis

In the Modal Analysis of the Model, we find 6 Mode Shapes of Free Vibrations to Find. To set this up, we create a Modal Analysis Project and link the Model of Static Structural to the Model of the Modal Analysis. This is done so that the Mesh, Composite Fabric, and Non-Composite Materials are kept the same. We are calculating the Natural Frequencies of the Airfoil for Every Mode Shape. In the Analysis Settings of Modal, input the value of “Max Modes to Find” as “6”. There is no requirement of changing other parameters under Modal.

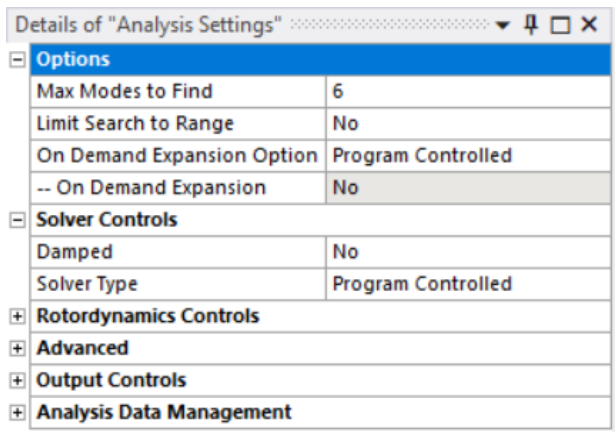

Details of "Analysis Settings"

Options	
Max Modes to Find	6
Limit Search to Range	No
On Demand Expansion Option	Program Controlled
-- On Demand Expansion	No
Solver Controls	
Damped	No
Solver Type	Program Controlled
Rotordynamics Controls	
Advanced	
Output Controls	
Analysis Data Management	

Figure 29: Details of Modal Pre-Analysis Settings

Final Project Schematic consisting of ACP, Static Structural and Modal Analysis:

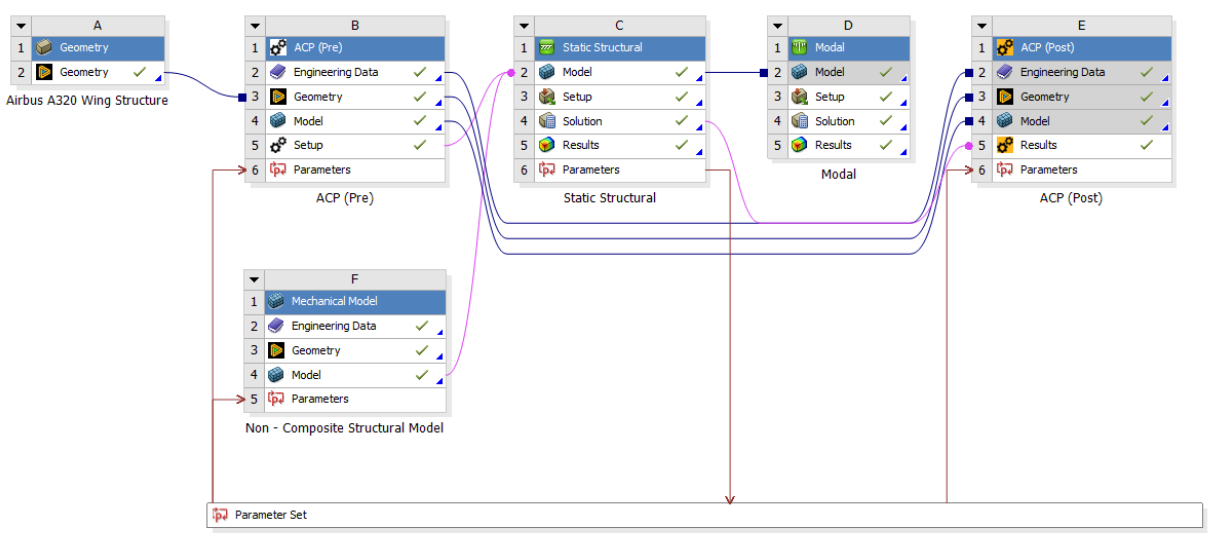

Figure 30: Project Schematic of ACP, Static Structural, Modal analyses

4.8 Explicit Dynamic Analysis (LS-DYNA)

Using the LS – DYNA Analysis System, we can conduct Explicit Dynamic Analysis on the Airfoil. This Explicit Dynamic Analysis is to crash the Airfoil into a concrete wall. This is done to visualize the process of driving the Composite Material of the Airfoil to Catastrophic Failure. Which helps us determine the final composite tolerable strength and compare it to the Reinforced composite fabrics.

In LS – DYNA of Ansys Workbench we need to map three different Models into the Model of LS – DYNA, which would be the Non-Composite Wing Structure of the Wing, Composite Fabric from ACP and the Model of the Wall made of concrete. The mesh of the concrete wall here is not of much importance due to the focus on the stresses and deformations in the wing and not on the wall.

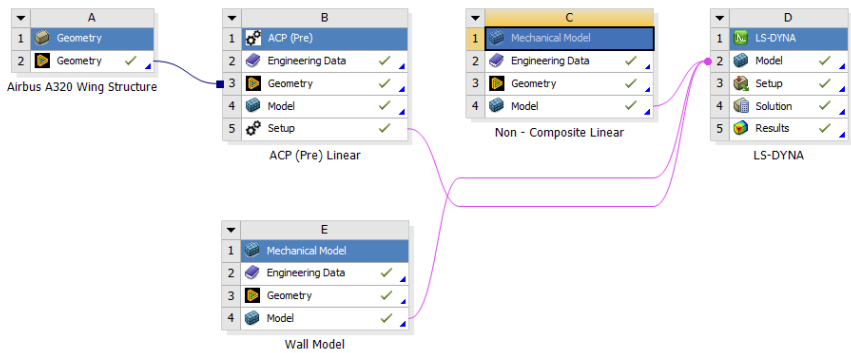

Figure 31: LS - DYNA Project Schematic

In the setup we set the Maximum Number of Cycles as 10e+6 and end time as 0.01s for the airfoil being 2m away from contact with wall. And an initial velocity V_{in} = 246 m/s is given. All other parameters are left as default.

Details of "Analysis Settings"

Step Controls	
End Time	0.01 s
Time Step Safety Factor	0.9
Maximum Number Of Cycles	1000000
Automatic Mass Scaling	No
Number of Cases	0
CPU and Memory Management	
Solver Controls	
Initial Velocities	
Initial Velocities are applied immediately	Yes
Damping Controls	
Hourglass Controls	
Composite Controls	
Advanced	
Output Controls	
Time History Output Controls	
Analysis Data Management	

Figure 32: LS - DYNA Analysis Settings

4.9 CNT Integration

In the final section of the project, CNTs are introduced into the composite material fabric, causing the material properties to change. This implies that the Static Structural Analysis, Modal Analysis, Explicit Dynamic Analysis (LS – DYNA) are to be run again with different material properties. And the results are to be evaluated.

Properties of Outline Row 3: Epoxy Carbon Woven (395 GPa) Prepreg

	A	B	C	D	E
1	Property	Value	Unit		
2	Density	1480	kg m^-3		
3	Orthotropic Secant Coefficient of Thermal Expansion				
8	Orthotropic Elasticity				
9	Young's Modulus X direction	9.182E+10	Pa		
10	Young's Modulus Y direction	9.182E+10	Pa		
11	Young's Modulus Z direction	9E+09	Pa		
12	Poisson's Ratio XY	0.05			
13	Poisson's Ratio YZ	0.3			
14	Poisson's Ratio XZ	0.3			
15	Shear Modulus XY	3.6E+09	Pa		
16	Shear Modulus YZ	3E+09	Pa		
17	Shear Modulus XZ	3E+09	Pa		
18	Orthotropic Stress Limits				
28	Orthotropic Strain Limits				
38	Tsai-Wu Constants				
42	Ply Type				

Figure 33: Pre CNT-Integration Material Properties

Properties of Outline Row 3: Epoxy Carbon Woven (395 GPa) Prepreg

	A	B	C	D	E
1	Property	Value	Unit		
2	Density	1480	kg m^-3		
3	Orthotropic Secant Coefficient of Thermal Expansion				
8	Orthotropic Elasticity				
9	Young's Modulus X direction	1.26E+11	Pa		
10	Young's Modulus Y direction	1.26E+11	Pa		
11	Young's Modulus Z direction	2E+10	Pa		
12	Poisson's Ratio XY	0.05			
13	Poisson's Ratio YZ	0.3			
14	Poisson's Ratio XZ	0.3			
15	Shear Modulus XY	6.64E+09	Pa		
16	Shear Modulus YZ	5.3E+09	Pa		
17	Shear Modulus XZ	5.3E+09	Pa		
18	Orthotropic Stress Limits				
28	Orthotropic Strain Limits				
38	Tsai-Wu Constants				
42	Ply Type				

Figure 34: Post CNT-Integration Material Properties

Chapter 5 - Results and Discussion

5.1 Fusion 360

Below shown are some renders of the 3D CAD Model file:

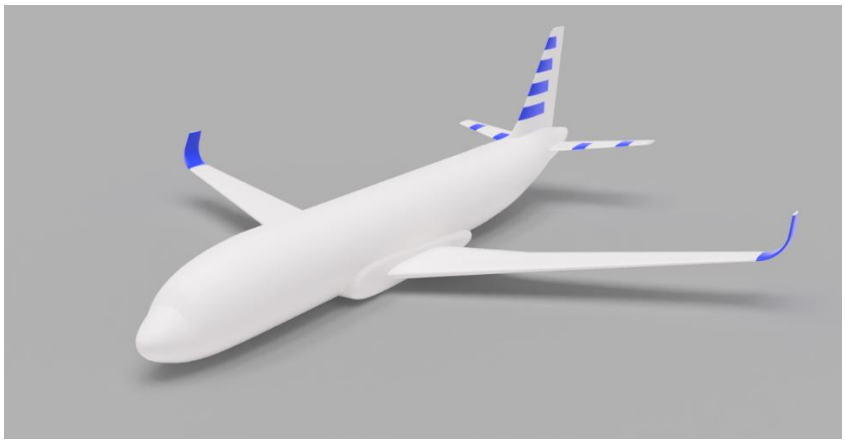

Figure 35: Isometric View

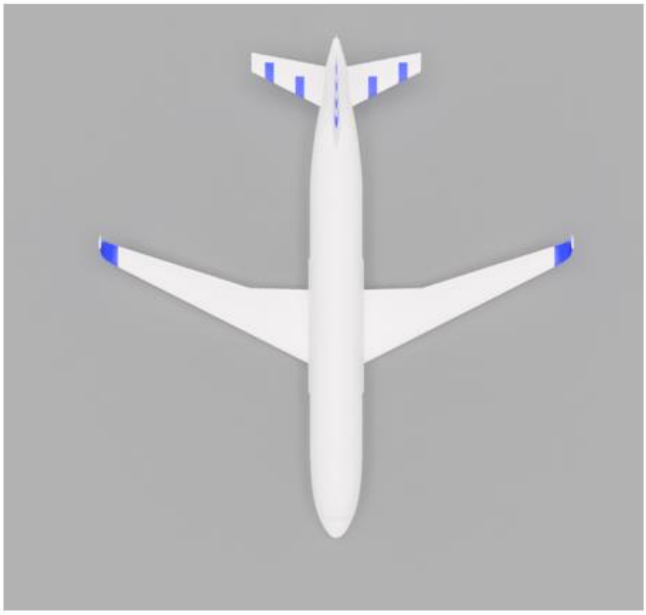

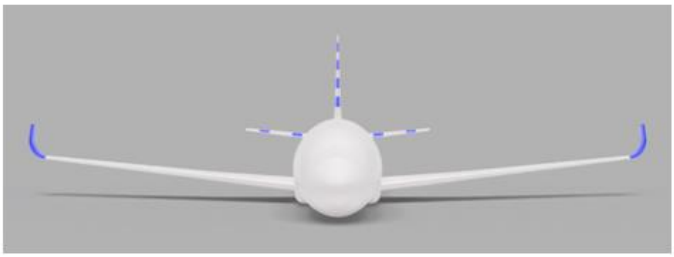

Figure 36: Top View and Front View

5.2 2D CFD Analysis

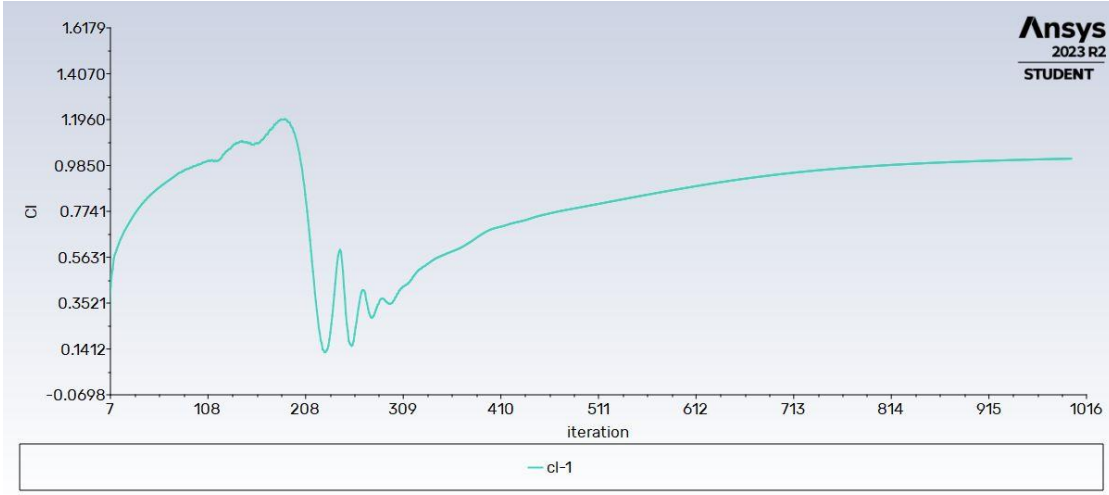

Figure 37: Coefficient of Lift

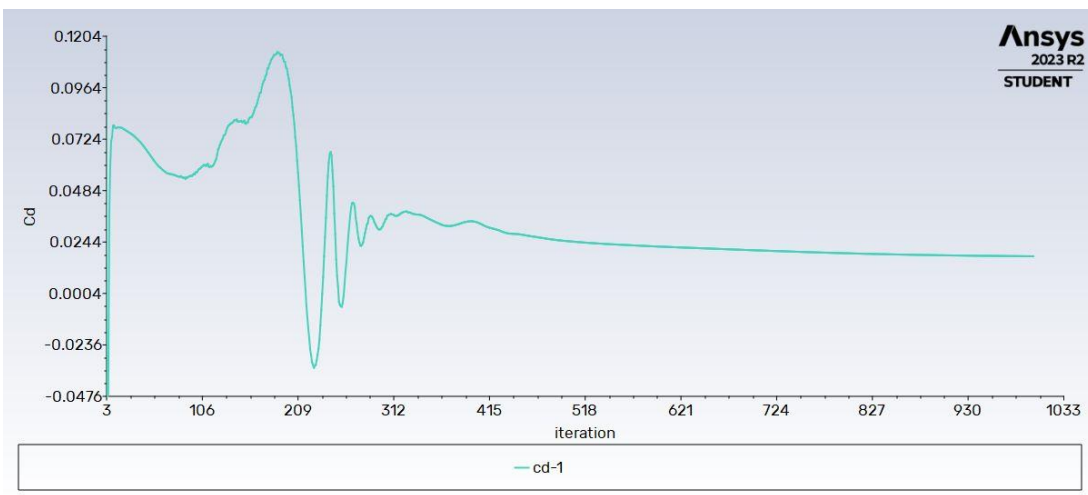

Figure 38: Coefficient of Drag

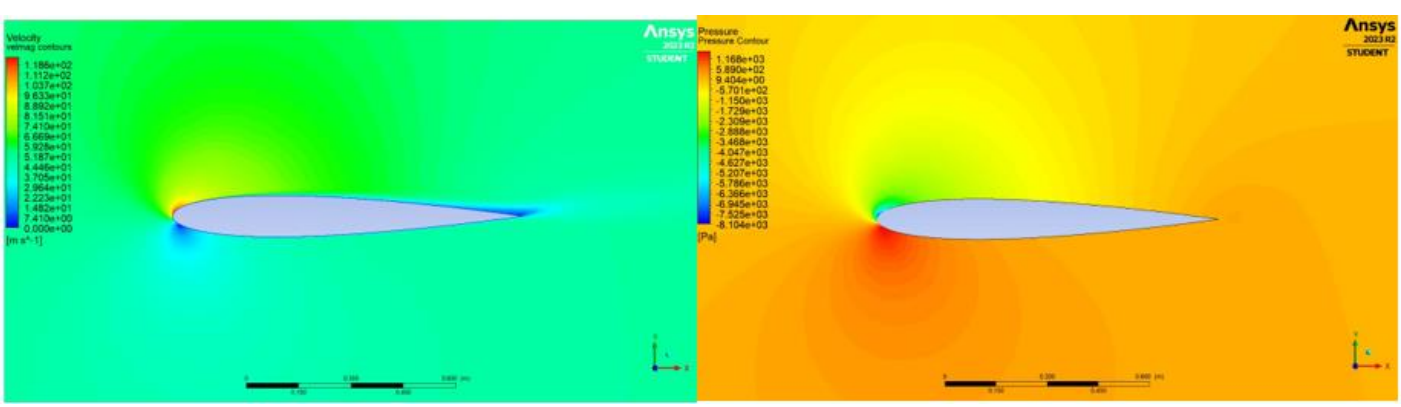

Figure 39: Velocity and Pressure Contours

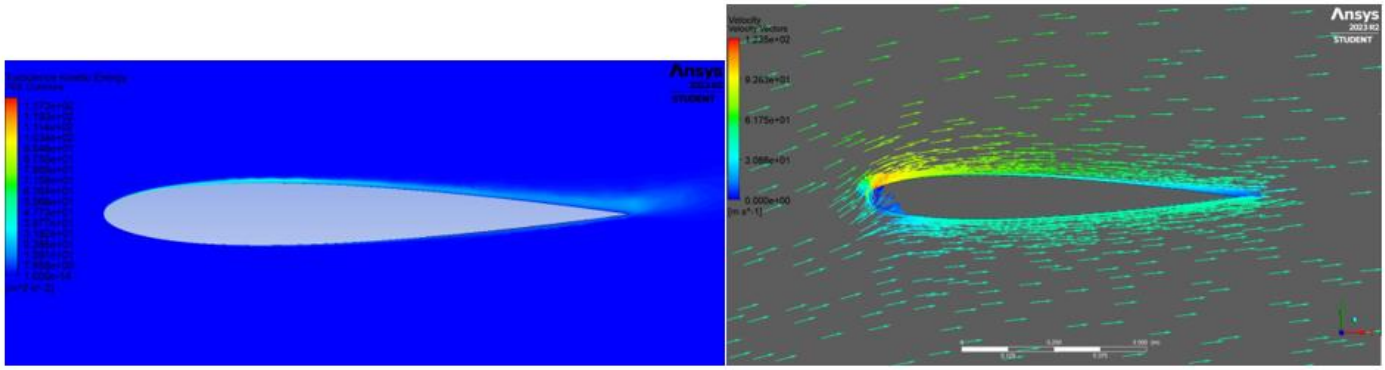

Figure 40: Total Kinetic Energy Contour and Velocity Vectors

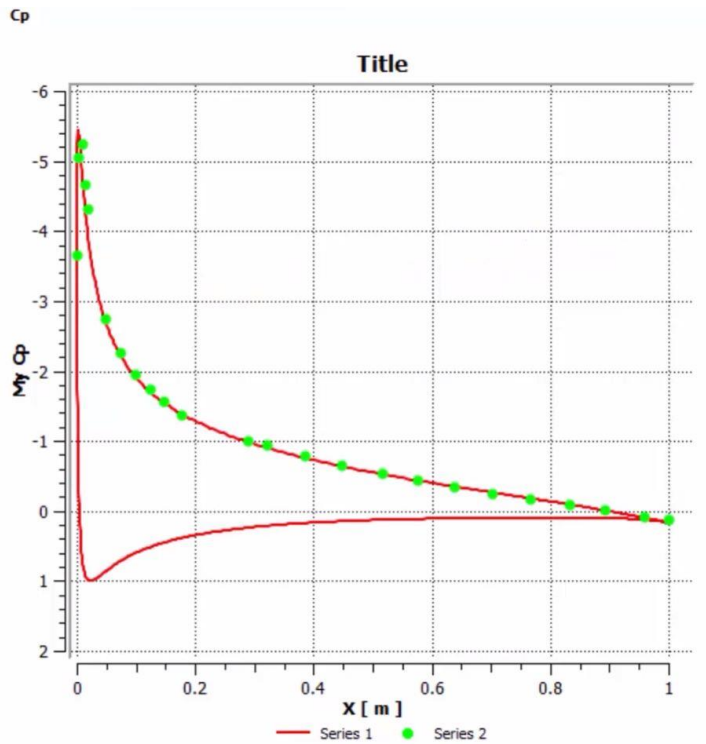

Figure 41: Plot of Cp with Experimental Validation

The Value of Cp has been Validated in *Figure 41*, and the validation of C_L and C_D can be seen as follows:

Experimental Validation		
Parameter	**Experimental**	**Analytical**
α (AOA)	10.12° – 10.18°	10°
C_L	1.07 – 1.08	1.06
C_D	0.012	0.016

Table 8: Validation Check

Hence, we can conclude that our mathematical model for the CFD Analysis of Airfoil is Reliable, and can proceed to 3D CFD Simulations.

5.3 3D CFD Simulations

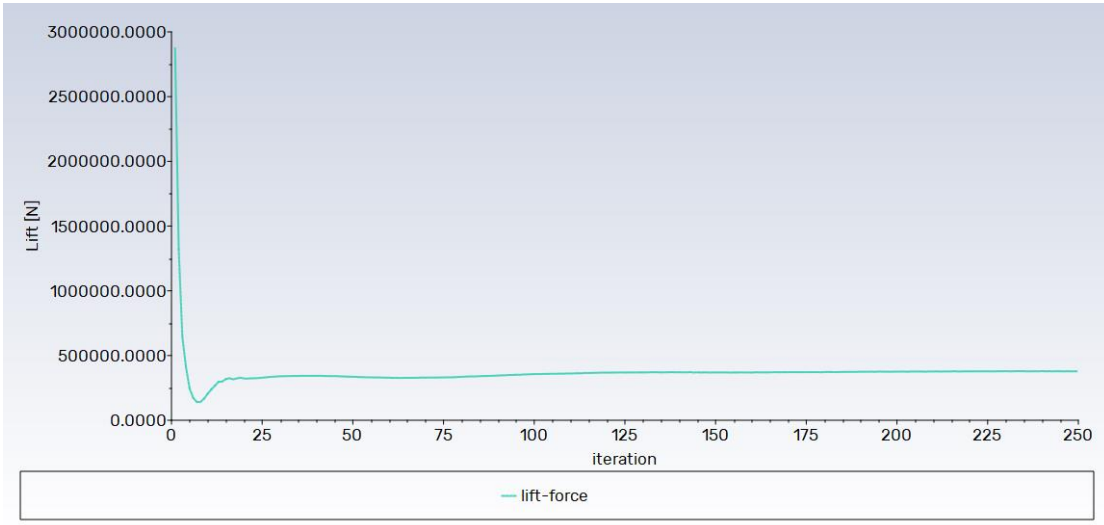

Figure 42: Lift Force vs. Iterations

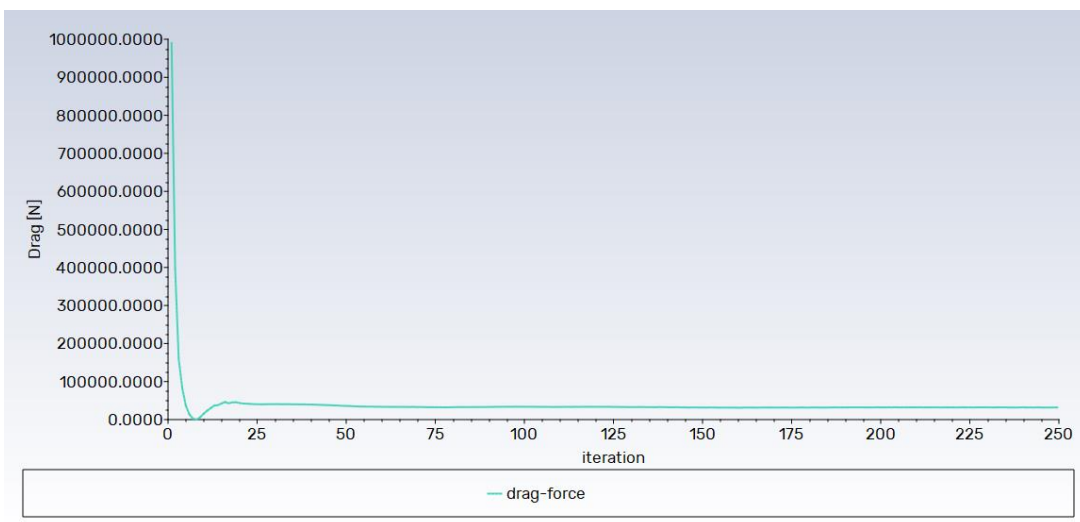

Figure 43: Drag Force vs. Iterations

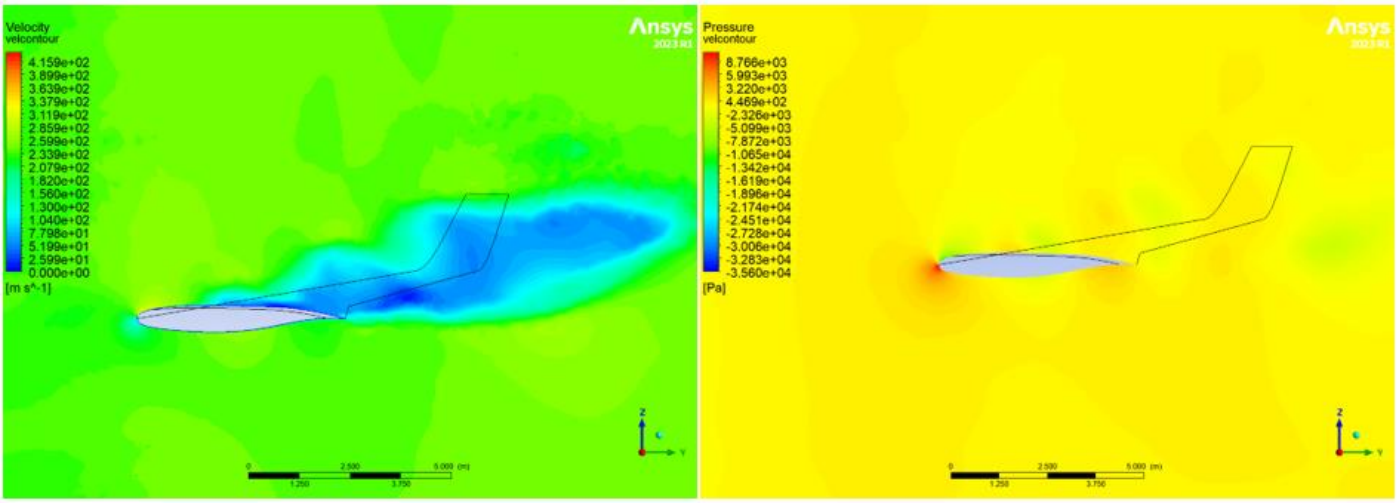

Figure 44: Velocity and Pressure Contours

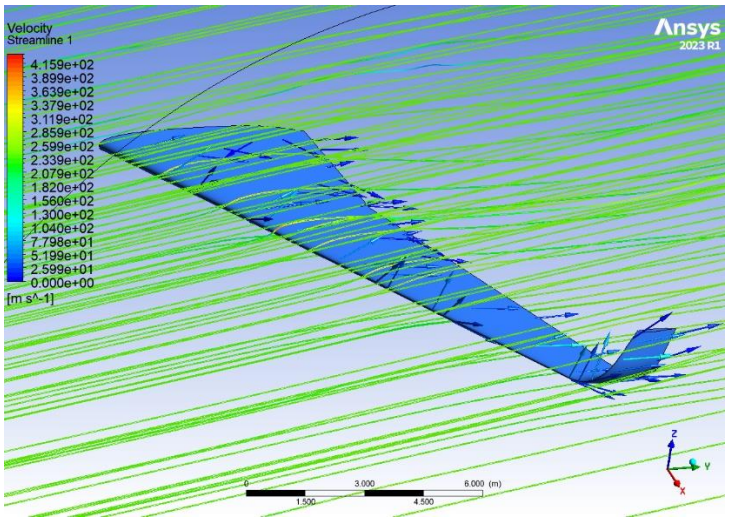

Figure 45: Streamlines

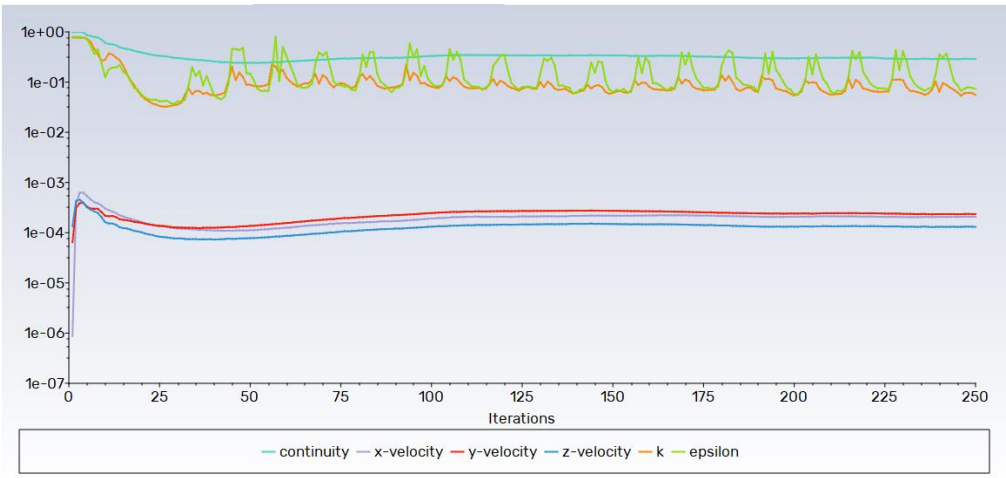

Figure 46: Scaled Residuals

Obtained 3D CFD Results		
Parameter		**Value**
Acting Forces	Lift Force	375.7 kN
	Drag Force	31 kN
Scaled Residuals	Continuity	0.75
	x-velocity	0.0004
	y-velocity	0.0005
	z-velocity	0.00015
	K	0.11
	Epsilon	0.09

Table 9: 3D CFD Results

5.4 CFD To FEA Verification

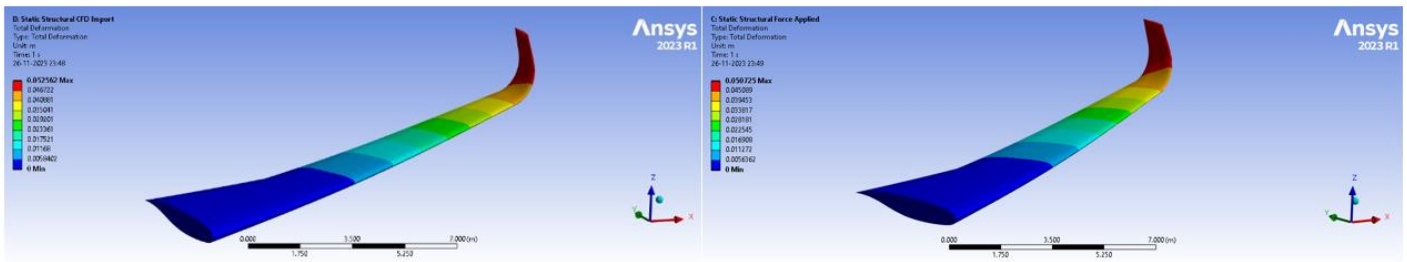

Figure 47: CFD And Manually Applied Force Deformation

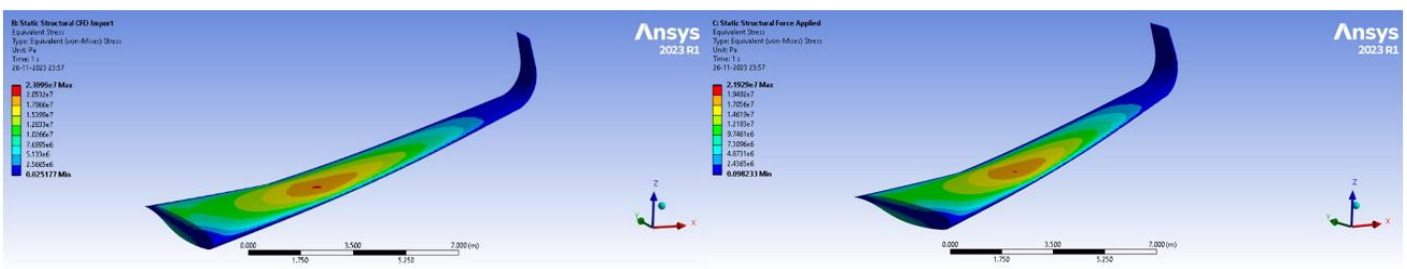

Figure 48: CFD And Manually Applied Force Stresses

CFD Applied and Manual Applied Parameter Comparison				
Parameter		**CFD**	**Manual**	**Conformity**
Total Deformation	Max.	5.2562e-002 m	5.0725e-002 m	96.5%
	Avg.	1.1183e-002 m	1.0714e-002 m	95.8%
Equivalent Stress	Max.	2.3099e+007 Pa	2.1929e+007 Pa	94.93%
	Avg.	6.3825e+006 Pa	6.1118e+006 Pa	95.76%

Table 10: CFD and Manual Application Parameter Comparison

Hence, we can be sure to manually apply Lift Force as a surface force in Finite Element Analyses.

5.5 ANSYS Composite PrePost

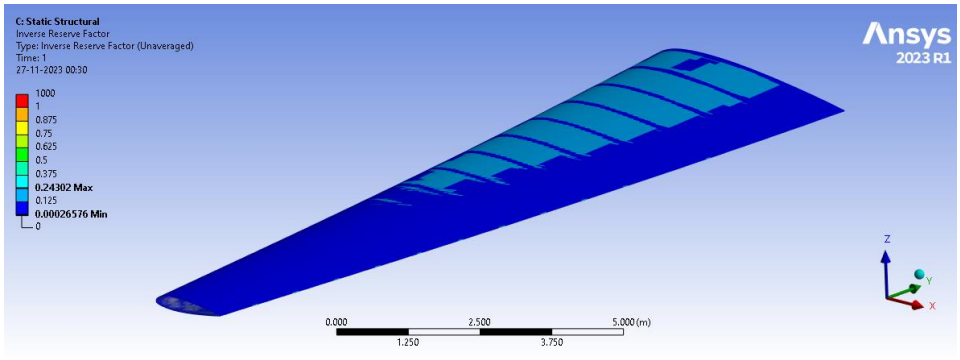

Figure 49: Inverse Reserve Factor

ACP Post Results				
Ply Type	**Parameter**	**Ply A**	**Ply B**	**Ply C**
Regular	Inverse Reserve	0.24	0.21	0.20
	Safety Factor	4.11	4.65	4.93
CNT Reinforced	Inverse Reserve	0.3	0.25	0.23
	Safety Factor	3.32	3.91	4.30

Table 11: ACP Post Results

The results here may misrepresent the strength of CNT Reinforced Plies. This is because IRF (Inverse Reserve Factor) and SF (Safety Factor) show with respect to Ply failure like De-Lamination, tensile, compressive or shear fracture of the matrix, bond failure of the fiber-matrix interface and tensile or compressive (buckling) failure of the fibers. This has very minimal correlation to Structural Strength of the Airfoil as a whole.

5.6 Static Structural Analysis

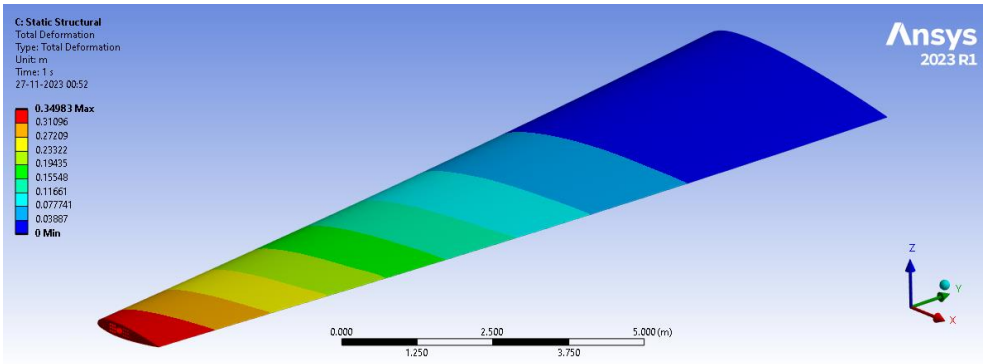

Figure 50: Total Deformation

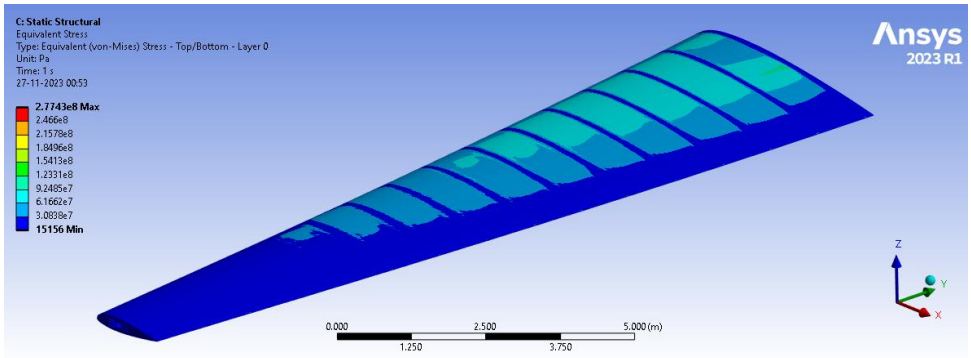

Figure 51: Equivalent Stresses

Static Structural Analysis Results				
Ply Type	**Parameter**	**Ply A**	**Ply B**	**Ply C**
Regular	Total Deformation	0.34 m	0.26 m	0.23 m
	Equivalent Stress	270 MPa	250 MPa	240 MPa
	Composite Stress	180 MPa	140 MPa	125 MPa
CNT Reinforced	Total Deformation	0.28 m	0.20 m	0.18 m
	Equivalent Stress	270 MPa	250 MPa	240 MPa
	Composite Stress	160 MPa	120 MPa	113 MPa

Table 12: Static Structural Analysis Results

From the Results we can see that there is about **18% - 25%** Reduction in the net maximum total deformation of the airplane wing, with some reduction in Equivalent stresses and a similar result in the stresses in the isolated composite fabrics of the airfoil. Hence, we can conclude that we find the ply to be about **18% - 25%** stronger than before.

5.7 Modal Analysis

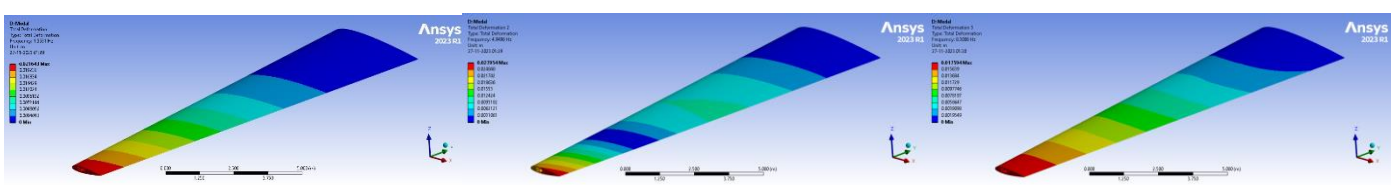

Figure 52: Mode Shapes 1, 2 and 3

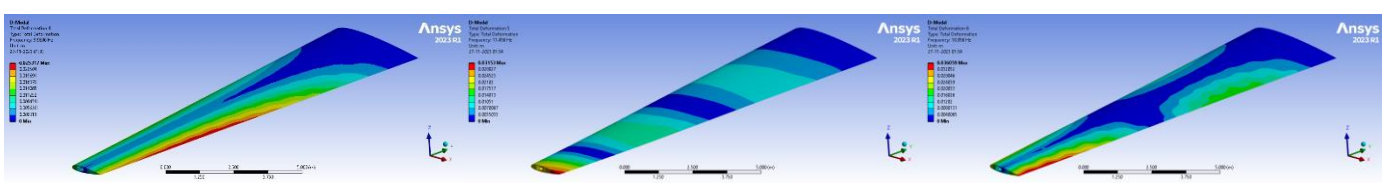

Figure 53: Mode Shapes 4, 5 and 6

Modal Analysis Results					
Type of Ply	**Mode Shape**	**Parameter**	**Ply A**	**Ply B**	**Ply C**
Regular	**1**	Deformation	0.021	0.021	0.020
		Frequency	1.35	1.5	1.56
	2	Deformation	0.028	0.025	0.025
		Frequency	4.95	5.56	5.81
	3	Deformation	0.018	0.019	0.019
		Frequency	8.30	9.94	10.23
	4	Deformation	0.025	0.026	0.026
		Frequency	9.96	12.94	13.53
	5	Deformation	0.031	0.024	0.023
		Frequency	11.46	15.13	16.68
	6	Deformation	0.036	0.026	0.025
		Frequency	18.95	23.26	24.31
CNT Integrated	**1**	Deformation	0.021	0.020	0.020
		Frequency	1.49	1.67	1.75
	2	Deformation	0.028	0.025	0.025
		Frequency	5.46	6.22	6.53
	3	Deformation	0.018	0.019	0.019
		Frequency	8.84	10.61	10.95
	4	Deformation	0.025	0.026	0.025
		Frequency	10.76	14.46	15.18
	5	Deformation	0.032	0.024	0.023
		Frequency	12.61	17.05	18.90
	6	Deformation	0.035	0.026	0.025
		Frequency	20.68	25.84	27.12

Table 13: Modal Analysis Results (Deformation in m and Frequency in Hz)

In Modal Analysis we don’t find a trend of properties to conclude. This is because Modal Analysis mainly tends to be based on the structural integrity provided by the non-composite material like the Titanium Alloy for the Spars and Aluminum Alloy for the Ribs. And changes in ply doesn’t contribute a great extent to changing the modal shapes of the natural frequency of the airfoils.

5.8 Explicit Dynamic Analysis

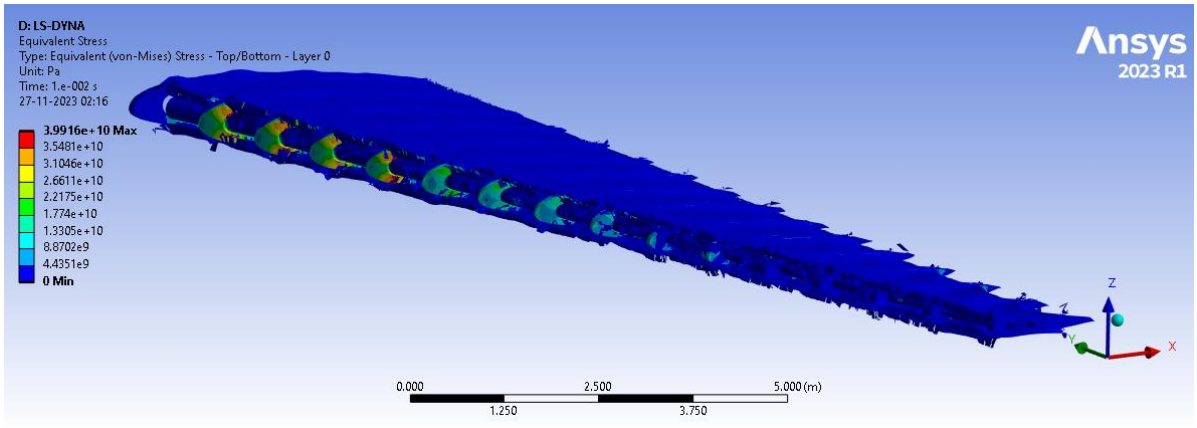

Figure 54: Equivalent Stress Contour at the End of Crash

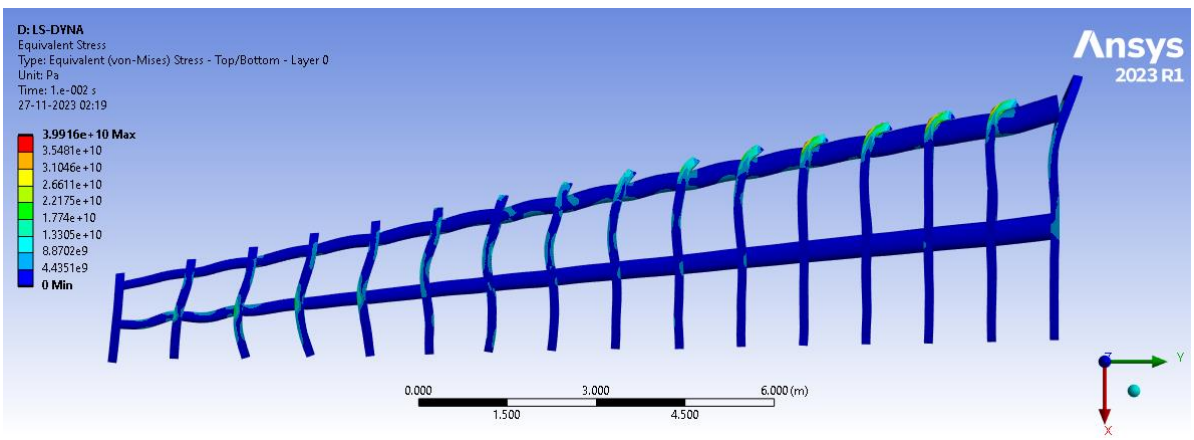

Figure 55: Stress Contour for Non-Composite Material

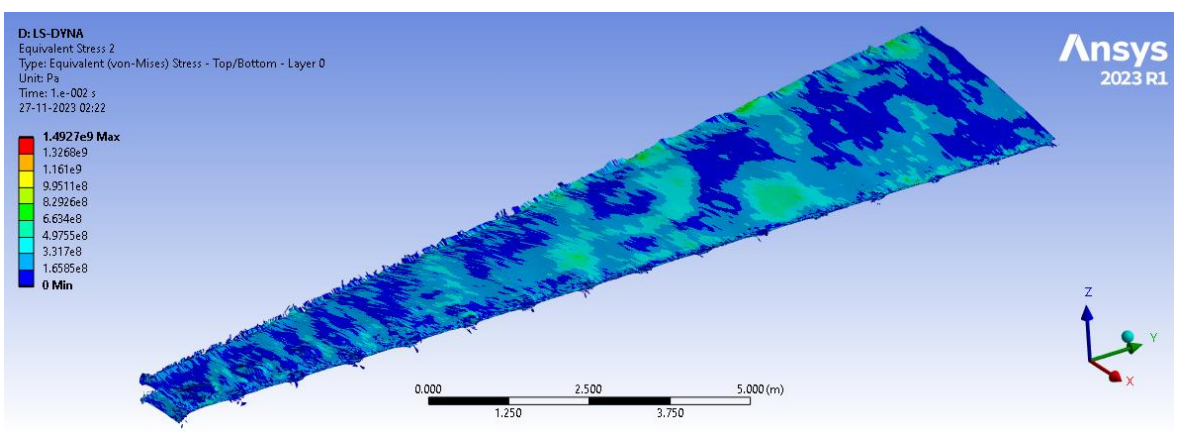

Figure 56: Equivalent Stresses for Composite Fabric

Explicit Dynamic Analysis Results				
Ply Type	**Equivalent Stress**	**Ply A**	**Ply B**	**Ply C**
Regular	Max.	1.8339 GPa	1.8106 GPa	1.6479 GPa
	Avg.	175.77 MPa	175.71 MPa	169.55 MPa
CNT Integrated	Max	1.5266 GPa	1.4972 GPa	1.4327 GPa
	Avg.	164.69 MPa	159.78 MPa	150.34 MPa

Table 14: Explicit Dynamic Analysis Results

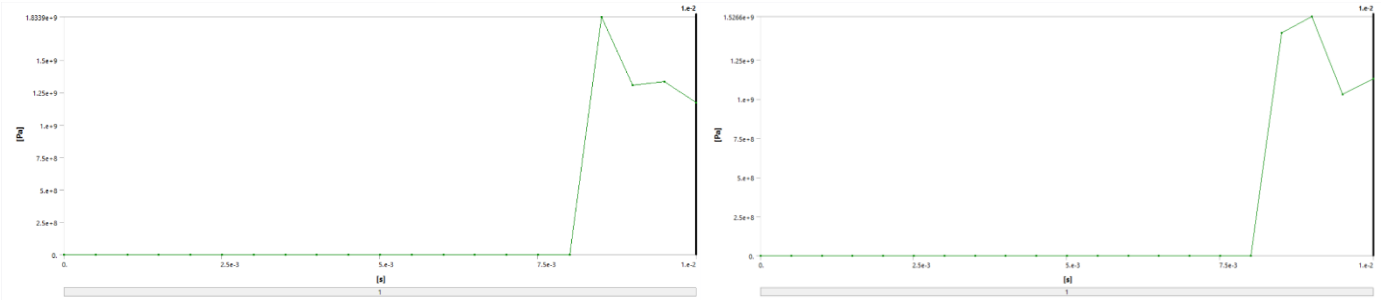

Figure 57: Ply A: Regular and CNT Integrated

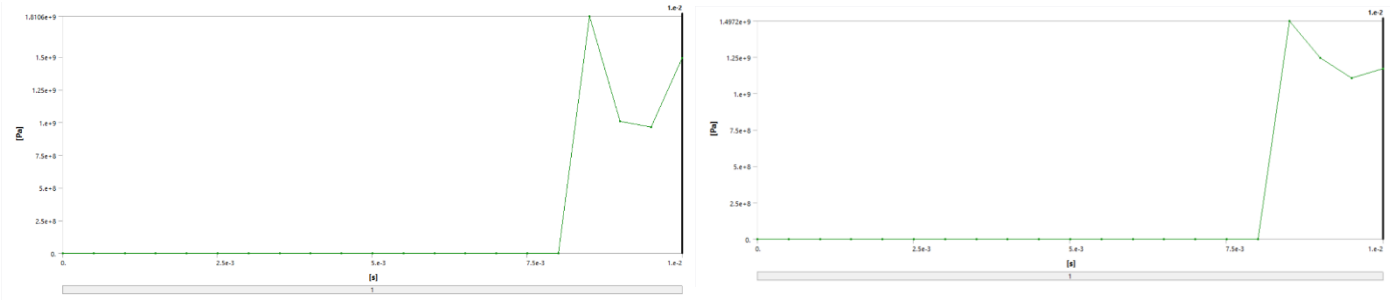

Figure 58: Ply B: Regular and CNT Integrated

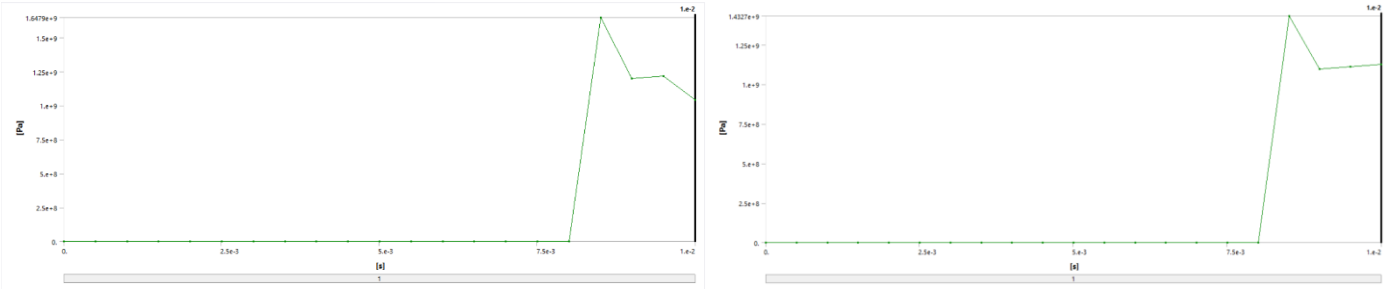

Figure 59: Ply C: Regular and CNT Integrated

Here Analyzing the different results of the Explicit Dynamic Analysis, we can see there is a **15% – 20%** change the stresses acting in every ply. We can also conclude that there is similar improvement in the strength of the fabric due to the inculcation of the CNTs. This also can be validated from publication [4].

Chapter 6 - Conclusion and Future Scope

6.1 Conclusion

In conclusion, the integration of Carbon Nanotubes (CNTs) into carbon fiber fabrics for airfoil construction demonstrates a significant enhancement in both explicit dynamic analysis tests and static structural tests, resulting in a commendable 15-25% increase in strength. This improvement can be attributed to the unique mechanical properties of CNTs, such as their exceptional tensile strength and stiffness. The explicit dynamic analysis tests reveal the ability of CNTs to enhance the material's resistance to dynamic loads, crucial for airfoils subjected to varying aerodynamic forces during flight. The addition of CNTs contributes to increased structural integrity and resilience, leading to improved performance and durability in challenging conditions.

Moreover, the static structural tests further underscore the positive impact of CNTs on the overall strength of the carbon fiber fabric. The CNT-infused composite material exhibits heightened resistance to deformation and increased load-bearing capacity, making it an ideal choice for airfoil applications where structural stability is paramount.

This significant strength improvement observed in both types of tests not only enhances the safety and reliability of airfoil structures but also opens ways for designing lighter and more efficient aircraft. The utilization of CNTs in carbon fiber fabrics not only meets but exceeds performance expectations, showcasing the promising potential of advanced composite materials in aerospace engineering. As the aviation industry seeks innovations for enhanced performance and fuel efficiency, the incorporation of CNTs in carbon fiber airfoils emerges as a compelling and forward-thinking solution.

We can also conclude that the integration of CNTs in carbon fiber airfoils, yielding a 15-25% strength increase, could also be crucial for preventing fatal crashes. Enhanced structural integrity ensures heightened resistance to dynamic forces, reducing the risk of catastrophic failures. This advancement in material science contributes significantly to aviation safety, potentially saving lives.

6.1.1 Static Structural Analysis

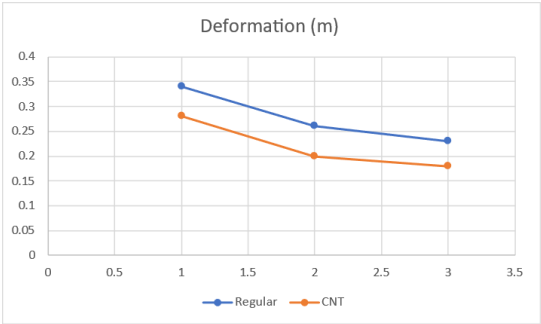

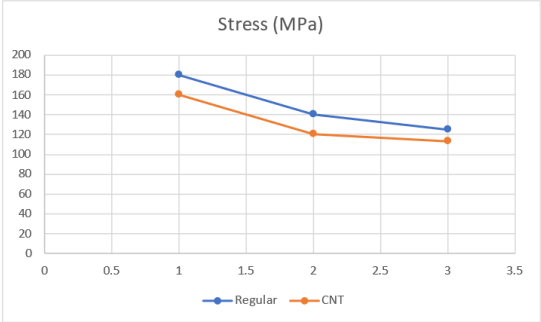

Figure 60: Static Structural Analysis Result Comparison

6.1.2 Explicit Dynamic Analysis

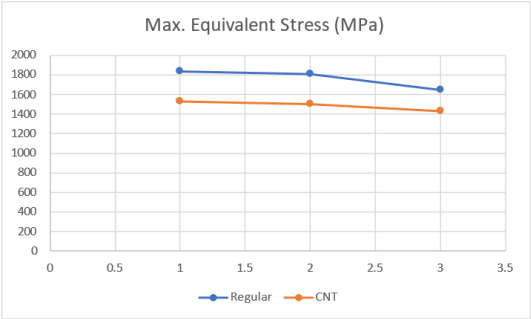

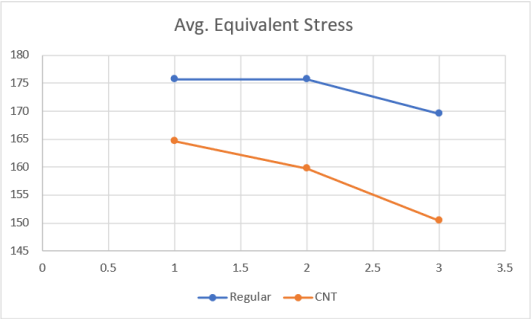

Figure 61: Explicit Dynamic Analysis Results Comparison

6.2 Future Scope

The future trajectory of aerofoils integrated with Carbon Nanotubes (CNTs) transcends conventional configurations by introducing "Wavy CNTs" causing further reinforcements in material strength. By exploring this approach, the aviation industry can revolutionize airfoil design, extending beyond the limits of traditional reinforcement. In this Paper however, only straight CNTs have been employed due to unavailability of required resources. The integration of "Wavy CNTs" offers a multi-dimensional enhancement of material strength, not only strengthening the airfoil in its primary axis but also providing increased resilience in secondary dimensions. This leap in structural integrity promises to redefine the capabilities of aerofoils, fostering greater efficiency and safety in aviation.

Reflecting on historical incidents, the potential impact of reinforced aerofoils becomes evident. Fatalities resulting from structural failures, particularly in critical flight phases, could have been averted with the implementation of CNT-reinforced materials. The added strength and durability offered by CNTs present a transformative solution, addressing vulnerabilities inherent in traditional materials and substantially mitigating the risk of catastrophic failures.

References

[1] Zakuan, M.A.M.B.M., Aabid, A. and Khan, S.A., 2019. Modelling and structural analysis of three-dimensional wing. International Journal of Engineering and Advanced Technology, 9(1), pp.6820-6828.

[2] Nath, A., Anand, R., Desai, J., Sultan, M.T.H. and Raj, S.A., 2021, September. Modelling and Finite Element Analysis of an Aircraft Wing using Composite Laminates. In IOP Conference Series: Materials Science and Engineering (Vol. 1183, No. 1, p. 012006). IOP Publishing.

[3] Vani, P.S., Reddy, D.R., Prasad, B.S. and Shekar, K.C., 2014. Design and analysis of A320 wing using E-glass epoxy composite. Int J Eng Res Technol, 3(11), pp.536-539.

[4] Das, S.K. and Roy, S., 2018, August. Finite element analysis of aircraft wing using carbon fiber reinforced polymer and glass fiber reinforced polymer. In IOP conference series: Materials science and engineering (Vol. 402, No. 1, p. 012077). IOP Publishing.

[5] Gupta, M., Patil, N.D. and Kundalwal, S.I., 2023, July. Influence of CNT waviness on the effective young's modulus of multiscale hybrid composite. In AIP Conference Proceedings (Vol. 2745, No. 1). AIP Publishing.

[6] Gupta, M., Ray, M.C., Patil, N.D. and Kundalwal, S.I., 2023. Effect of orientation of CNTs and piezoelectric fibers on the damping performance of multiscale composite plate. Journal of Intelligent Material Systems and Structures, 34(2), pp.194-216.